Published in final edited form as:
Nano Today. 2013 June ; 8(3): 290–312. doi:10.1016/j.nantod.2013.04.007.

Nonporous Silica Nanoparticles for Nanomedicine Application

Li Tang and **Jianjun Cheng***
Department of Materials Science and Engineering, University of Illinois at Urbana–Champaign, Urbana, Illinois, 61801, USA

Summary

Nanomedicine, the use of nanotechnology for biomedical applications, has potential to change the landscape of the diagnosis and therapy of many diseases. In the past several decades, the advancement in nanotechnology and material science has resulted in a large number of organic and inorganic nanomedicine platforms. Silica nanoparticles (NPs), which exhibit many unique properties, offer a promising drug delivery platform to realize the potential of nanomedicine. Mesoporous silica NPs have been extensively reviewed previously. Here we review the current state of the development and application of nonporous silica NPs for drug delivery and molecular imaging.

Keywords

Nanomedicine; nonporous silica nanoparticles; biomaterials; drug delivery; gene delivery; molecular imaging; nanotoxicity

Introduction

Nanomedicine, the use of nanotechnology for medical applications, has undergone rapid development in the last decade [1–8]. The goal of nanomedicine is to design and synthesize drug delivery vehicles that can carry sufficient drug loads, efficiently cross physiological barriers to reach target sites, and safely and sustainably cure diseases. Numerous organic nanomedicines, including liposomes, drug–polymer conjugates, dendrimers, polymeric micelles and nanoparticles (NPs), have been extensively studied as drug delivery systems (Fig. 1). Each delivery platform has its advantage and disadvantage. For example, high drug loadings have been achieved in liposomes [9], but the intrinsic structural stability of liposomes is undesirably low, especially under fluid shear stress during circulation. Inorganic drug delivery systems, such as gold NPs, quantum dots (QDs), silica NPs, iron oxide NPs, carbon nanotubes and other inorganic NPs with hollow or porous structure, have emerged as promising alternatives to organic systems for a wide range of biomedical applications (Fig. 2), among which silica NPs have attracted significant interest because of their unique properties amenable for in vivo applications [10, 11], such as hydrophilic surface favoring protracted circulation, versatile silane chemistry for surface functionalization, excellent biocompatibility, ease of large-scale synthesis, and low cost of NP production. In 2011, an Investigational New Drug Application for exploring an

*To whom correspondence should be addressed: Jianjun Cheng, Department of Materials Science and Engineering, University of Illinois at Urbana-Champaign, Urbana, IL 61801, USA. Tel.: 217-244-3924; Fax: 217-333-2736; jianjunc@illinois.edu.

ultrasmall nonporous silica NP for targeted molecular imaging of cancer was approved by the US Food and Drug Administration (FDA) for a first-in-human clinical trial [12, 13], highlighting the great potential and the most recent progress of clinical translation of silica NP drug delivery platform.

Silica NPs used for biomedical applications can be categorized as mesoporous or nonporous (solid) NPs, both of which bearing amorphous silica structure. Mesoporous silica NPs characterized by the meso-pores (2–50 nm pore size) are widely used for delivery of active payloads based on physical or chemical adsorption (Fig. 3a) [10, 14]. In contrast, nonporous silica NPs deliver cargos through encapsulation or conjugation (Fig. 3b. c). Payload release from mesoporous silica NPs can be controlled by using the “gatekeeper” strategy or modifying the inner surface of the pores to control the binding affinity with drugs (Fig. 3a) [10], whereas the release profile of payloads delivered by nonporous silica NPs are controlled by means of chemical linkers or the degradation of silica matrix (Fig. 3b. c). The size and shape of nonporous silica NPs can be excellently controlled, and the pore size and structure of mesoporous silica NPs can be controlled by tuning the composition and concentration of surfactants during synthesis. The nanomedicine applications of mesoporous silica NPs have been extensively reviewed elsewhere [10, 14–17] and are not discussed here. We also do not discuss the use of silica as a host material for other types of functional NPs (e.g., gold NPs, quantum dots and iron oxide NPs) to form hybrid NPs. This important class of silica-based hybrid nanomedicines has been thoroughly reviewed by Piao et al. [18]. Here, we focus on nonporous silica NPs and their biomedical applications for disease diagnosis and therapy. We will first discuss the synthesis of various nonporous silica NPs, including the methods developed to control the size, shape and surface properties of silica NPs. Their biomedical applications for both therapy and diagnosis will then be discussed. These applications are categorized based on the different active cargoes delivered by silica NPs: drug delivery for small molecule drugs, proteins, or photosensitizers, gene delivery, molecular imaging for incorporating different contrast agents. Finally, the safety and toxicity of silica NPs both *in vitro* and *in vivo* will be discussed, which is important for their potential clinical translation.

Synthesis and control of the properties of silica NPs

Many efforts have been made to prepare silica NPs with precisely controlled physicochemical properties. The excellent control over syntheses is the prerequisite for the biomedical application of silica NPs.

Size control

Synthesis of size-controlled silica NPs was first reported by Stöber, Fink, and Bohn in 1968 [19]. Monodisperse silica spheres with uniform diameters ranging from 50 nm to 2 μm were successfully prepared in a reaction mixture of water, alcoholic solvent, ammonia, and tetraalkoxysilane (Stöber method; Fig. 4). The effects of various alcoholic solvents and tetraalkoxysilanes, as well as the concentration of each component, on the reaction rates and particle sizes were systemically studied. The reaction parameters and mechanism were subsequently investigated by Bogush et al. and Van Blaaderen et al. and others [20, 21]. They demonstrated that the growth proceeds through a surface reaction-limited condensation of hydrolyzed monomers or small oligomers. The particle formation (or particle nucleation) proceeds through an aggregation process of siloxane substructures that is influenced strongly by the surface potential of the silica particles and the ionic strength of the reaction medium. Thus, the stability behavior of the silica nanoparticles in alcohol, water, and ammonia mixtures and the dependence of the rate constants of hydrolysis and condensation as a function of the reaction mixture play the most important role in determining the final silica NP sizes [21].

A seeded regrowth strategy was explored to improve the size control for larger NPs [20, 22]. The smallest NPs that can be prepared by the Stöber method without aggregation have diameters of 15–20 nm and are more polydisperse (typically 10–20% standard deviation) than larger NPs (< 3% standard deviation for NPs larger than 200 nm) [22–24]. Recently, in an important breakthrough, Hartlen et al. and Yokoi et al. prepared monodisperse silica NPs with diameters as small as 12 nm in a heterogeneous reaction with lysine or arginine instead of ammonia as a basic catalyst in the aqueous medium and tetraethoxysilane in the organic layer [25–27]. In another modification of the Stöber method, silica NPs were prepared in an aqueous microemulsion with added surfactants [28–31]. For example, the Prasad group prepared organically modified 30-nm silica-based NPs in a emulsion system with Aerosol OT surfactant [30, 31]; Meng et al. reported the formulation of 20- to 300-nm silica NPs in a water-based emulsion with sodium dodecylbenzene sulfonate as the surfactant [29].

An alternative method for the production of monodisperse silica spheres with diameters ranging from tens to a few hundreds of nanometers involves the use of reverse microemulsions, in which particles form in inverse micelles compartmentalized by a suitable surfactant in a nonpolar organic solvent [32]. This approach works particularly well for monodisperse NPs smaller than 100 nm in diameter [33–39] and permits easy encapsulation of active molecules in the micelles during NP formation. For example, Bagwe et al. and Jin et al. reported the synthesis of dye-doped silica NPs with continuously tunable sizes in a reverse microemulsion and used them for cellular contrast imaging [40, 41]. This method has also been widely used for coating other functional NPs with silica to produce core–shell structures, as summarized in an excellent review by Guerrero-Martinez et al [42].

Shape control

The shape of NPs dramatically affects their blood circulation [43] and tumor penetration behavior [44]. It has been reported that worm-like micelles have superior circulation times compared to spheric micelles likely due to the enhanced evasion of phagocytosis [43]. It is also noticeable that nanorods penetrate tumor tissues more rapidly than nanospheres likely because of improved transport through pores [44]. These results suggest the importance of controlling the shape of nanomedicine for favored circulation or tissue penetration properties.

Although there are many methods for the size-controlled preparation of silica nanospheres, only a handful of methods have been reported for the preparing of one-dimensional silica nanorods/nanotubes [45–50] and other nanostructures [51–55]. The methods for shape control of silica NPs are mainly using templates [45, 46, 51, 52] or through polymer adsorption [49]. For example, silica nanotubes can be prepared with various templates, including anodic aluminum oxide membranes [46, 47], cylindrical polymer brushes [48], and nickel-hydrazine complex nanorods [50]. Recently, Kuijk et al. reported the polyvinylpyrrolidone-mediated synthesis of monodisperse silica nanorods with tunable aspect ratio in an emulsion system (Fig. 4) [49]. Interestingly, hollow silica nanospheres [51, 53, 55] and nanorattles [52, 54] with well-defined structures have also been prepared, and their application for delivery of anticancer drugs, proteins, or DNA have been explored. This facile shape control of silica NPs is important for fundamental studies of understanding the shape effect of nanomedicine in biological system and for clinical applications of optimizing the shape of nanomedicine for improved diagnosis and therapy.

Surface property control

The surface properties of NPs are known to play an important role in determining the interactions between NP and biological system (e.g., cellular internalization and trafficking, biodistribution and tumor penetration of NPs) [56–58]. Therefor, to achieve efficient disease

targeting and improved therapy, it is important to modulate the surface properties of any nanomedicines. Silica NP has the advantage of easy surface modification via physical adsorption or covalent conjugation using silane chemistry. Depending on the specific application, the surface property of silica NP could be easily tuned. For example, surface charge of silica NP can be easily controlled with the addition of 3-aminopropyltriethoxysilane, 3-(trihydroxysilyl)-propylmethylphosphonate or carboxyethylsilanetriol, or zwitterion silanes following the formulation of silica NPs. As a result, silica NPs with positive, negative, or zwitterionic surface charge could be prepared (Fig. 4) [59–62]. In fact, many other different functional groups could be grafted to the silica NP surface using similar method because there are a large number of these silane compounds available commercially [59, 63].

In addition, silica NP surface can be functionalized with polymers either chemically (through covalent bonding) or physically (by physical adsorption) (Fig. 4). The former is favored due to the stable covalent bonding between the polymer and NP. For example, polyethylene glycol (PEG) can be conjugated to silica NP surface via a “grafting-to” method [59, 64–67]. On the other hand, “grafting-from” method has also been employed for the surface modification of silica NPs [68]. Jia et al. grafted silica NP surface with biocompatible and functionalizable zwitterionic poly[[3-(acryloylamino)propyl](2-carboxyethyl)dimethylammonium] via surface initiated atomic transfer radical polymerization [69]. A number of polymerization techniques have been applied for surface initiated polymerization on silica NPs, as summarized in an excellent review by Radhakrishnan et al [70].

The surface of silica NPs can also be functionalized with various targeting ligands (Fig. 4), for example, antibodies or aptamers [71–75]. In summary, due to the versatile silane chemistry, many functional moieties could be conjugated to the silica NP surface. Thus, many desired surface properties for biomedical applications could be easily obtained using silica NP, which is critical for developing targeted nanomedicine for various diseases.

Silica NPs for drug delivery

The use of silica materials for delivery and controlled release of drug payloads was reported as early as 1983 [76]. Since then, silica NPs have been extensively used as drug carriers, owing to their biocompatibility and easy formulation with drugs. Initially, silica was used mainly in the form of xerogels loaded with bioactive reagents [77]. For example, silica xerogels have been used as implantable carrier for controlled drug release [78, 79]. Silica NPs emerged as a popular drug delivery system about 10 years later [11]. A wide range of different kinds of payloads, including small-molecule drugs, photosensitizers for photodynamic therapy (PDT), proteins, peptides, DNAs and RNAs, have been incorporated into silica NPs to target diseases such as cancer, heart disease [80, 81], and Parkinson’s disease [82]. Using silica NPs to deliver bioactive molecules can protect them from degradation under physiological conditions, allow for controlled release, prolong their blood circulation, improve disease targeting, and minimize side effects to healthy tissues. Depending on the properties of the cargoes delivered, different formulation strategies were used for preparing silica nanomedicines.

Small-molecule drug delivery

There are two general strategies for incorporating small-molecule drugs into silica NPs: encapsulation and conjugation (Fig. 3b, c). The former strategy involves the preparation of silica NPs with hollow structures, into which drugs are loaded after NP formation (Fig. 3b); this is one of the methods for encapsulation [46, 51–54, 83–85]. This process results in a non-covalent binding between drug and silica matrix, which is similar to that used for

adsorption of drugs in meso pores of mesoporous silica NPs. The active molecules can also be encapsulated in the silica matrix during NP formation [86–95]. In contrast, the conjugation strategy involves linking drugs and silica NPs via covalent bonds (Fig. 3c).[30, 96–105]

Silica NPs are formed by a sol–gel process, a two-step inorganic polycondensation reaction consisting of hydrolysis and condensation. Adding bioactive molecules during oxide backbone formation facilitates their encapsulation within the oxide matrix, leading to the production of a composite with the active ingredients trapped inside the resulting silica materials. This strategy is frequently employed for preparing silica xerogels encapsulating a range of bioactive molecules [88–93]. Tailoring the properties of the nanostructure (e.g., density and pore size) by controlling the sol–gel reaction kinetics allows for the control of the release kinetics of the encapsulated molecules [11]. For example, introducing an acid or base during the hydrolysis and condensation markedly changes the xerogel microstructure, which in turn changes the release kinetics. Release occurs by a combination of diffusion of the encapsulated molecules and dissolution of the silica matrix. Silica implants dissolve over time under physiological conditions [11, 78, 106], as will be discussed in later section (Safety an Toxicity). The strategy has also been explored for preparation of drug-encapsulating silica NPs for cancer therapy [94, 95]. For example, He et al. encapsulated doxorubicin in silica NPs via reverse microemulsion method [95]. Drug loading and entrapment efficiency is 4.2 ± 0.3% and 22.0 ±3.6%, respectively.

Drugs have been loaded into silica NPs with hollow structures, including nanospheres and nanotubes. Tang group synthesized silica nanorattles, which have unique ball-in-ball structure and can deliver the antitumor drugs, docetaxel and doxorubicin [52, 54, 107, 108]. Compared to Taxotere®, this formulation of docetaxel shows a ~15% higher tumor inhibition efficiency in the murine hepatocarcinoma 22 subcutaneous tumor model. Deng et al. developed hollow silica–chitosan hybrid NPs for delivery of tumor necrosis factor alpha (TNF-α) for cancer therapy [51]. These silica NPs, with their pH-sensitive cationic polysaccharide-chitosan surface coating, permit controlled release of the drug payload in pericellular and interstitial environment to suppress the growth of cancerous cells. Yan et al. developed similar hollow silica–chitosan hybrid nanospheres loaded with doxorubicin and demonstrated their *in vivo* antitumor efficacy [53]. Silica nanotubes derived from $Gd(OH)_3$ nanorods can be loaded with camptothecin for potential oral delivery based on their pH-dependent degradability [109].

Silica cross-linked micelles [110, 111] or microcapsulates [112] represent another interesting drug delivery system, in which the instability of conventional micelles is overcome by the addition of a silica shell on the micelle surface. These micelles or microcapsules, are usually hybrids of silica and polymers or lipids. For example, Huo et al. prepared a new class of robust, ultrafine silica core–shell NPs from silica cross-linked, individual block copolymer micelles [111]. These hybrid micelles show substantially improved stability upon dilution and slower release of their payload compared to non-cross-linked micelles. Tan et al. reported a silica–lipid hybrid microcapsule system for oral delivery of the poorly water-soluble drug, celecoxib; the formulation enhances *in vitro* dissolution and *in vivo* absorption of the drug [112].

Various covalent conjugation strategies for loading drugs in silica NPs have been explored. For example, the Schoenfisch group reported nitric oxide (NO)–releasing silica NPs with tunable sizes and drug release kinetics [98]. These NPs exhibit enhanced inhibition of ovarian tumor cells as compared to both control NPs and a previously reported small-molecule NO donor (pyrrolidine/NO). In addition, the NO-releasing NPs show greater inhibition effect on the anchorage-independent growth of tumor-derived and Ras-

transformed ovarian cells.[96] In addition, bleomycin-A5, an anticancer drug that chelates metals such as Fe(II) and catalyzes the formation of single-stranded or double-stranded DNA lesions in the presence of oxygen, maintains its cytotoxicity when it is conjugated to the surface of silica NPs [97]. Recently, novel conjugation strategies have emerged to incorporate small-molecule anticancer drugs to silica NP using the silane chemistry. The Lin group reported the development of bridged polysilsesquioxane nanoparticles for oxaliplatin delivery [103]. In their approach, the bis(trialkoxysilanes) monomer containing a Pt(IV) complex was first synthesized, and then hydrolyzed and condensed to form polysilsesquioxane NPs through base-catalyzed sol–gel polymerization in an anionic reverse microemulsion system (Fig. 5a). Much higher drug loading capacity was achieved (35–47% by weight) compared to other known nanoparticle platforms that deliver Pt(IV) prodrugs. The Pt(IV) prodrug in polysilsesquioxane NPs can be rapidly reduced in physiological condition by endogenous biomolecules, such as glutathione and cysteine, to release the active Pt(II) complex and bind DNA (Fig. 5a). The improved anticancer efficacy was demonstrated *in vivo* in an AsPC-1 pancreatic subcutaneous xenograft tumor model in mouse.

Our group recently developed a potentially clinically applicable drug-silica nanoconjugate system with excellent control over NP size and drug loading and release process [104]. The trialkoxysilane-containing drugs were synthesized with a degradable ester linker between drug and trialkoxysilane group and then condensed with tetraalkoxysilane to allow the drug molecules to be incorporated into the resulting silica NPs; the drugs can be released through the cleavage of the ester linker (Fig. 6a). By carefully controlling Stöber reaction conditions, we were able to prepare pyrene-silica nanoconjugates with controlled monodisperse sizes (less than 10% coefficient of variation, the ratio of the standard deviation to the mean of particle size) ranging from 20 to 200 nm as a proof of concept (Fig. 6b). Anticancer drugs (e.g., camptothecin, paclitaxel, docetaxel) or fluorescence dyes (e.g., rhodamine, IR783) conjugated silica NPs with precisely controlled sizes can be prepared similarly (Fig. 6a). The drug-silica nanoconjugates exhibited high drug loading (10–20%) and tunable drug release profiles, and can be easily prepared on gram scale but still with perfectly controlled sizes and mono-disperse size distribution. Such excellently size-controlled drug delivery nanomedicine allows us to systematically evaluate the size effect of nanomedicine on *in vivo* biodistribution, tumor tissue penetration (Fig. 6c) and cellular internalization, as well as the overall antitumor efficacy, through which we could gain fundamental understanding of the correlation between physiochemical properties of nanomedicines and their interaction with biological systems for potential clinical biomedical applications [104, 105].

Protein delivery

Protein and peptide biopharmaceuticals commonly suffer from pharmacokinetic and pharmacological drawbacks such as short circulating half-lives, immunogenicity, instability to proteolytic degradation, and low solubility. Therefore, a delivery system that improves the efficacy of protein drugs is highly desired. Silica has long been used to trap enzymes for biocatalysis because of the many advantages of silica NPs, for example, the ease of NP formation, matrix degradability, stability, and tunability of physicochemical properties of silica NPs. The Zink group did the pioneering work on encapsulation of various proteins, including copper-zinc superoxide dismutase, cytochrome c, and myoglobin, in transparent silica glass, and these investigators demonstrated that the encapsulated biomolecules maintain their characteristic reactivities and spectroscopic properties [113]. The use of silica NPs to immobilize enzymes for biocatalysis was comprehensively reviewed by Betancor et al. [114], so here we focus on silica NP–based systems for delivery of protein therapeutics and drug analogs.

Proteins can be either encapsulated in the silica NP matrix or adsorbed on or conjugated to the NP surface. The Mann group reported the feasibility of wrapping a single molecule of met-myoglobin within silica NPs by means of a reverse microemulsion method, by which uniformly sized silica NPs that trap proteins can be readily prepared without loss of protein structure or function. In addition, the trapped proteins show enhanced thermal stability [87]. Recently, Cao et al. reported an improved method for encapsulating a His-tagged protein by reverse microemulsion with the addition of a small amount of Ca^{2+} during NP formation to strengthen the binding between the protein and the silica shell [86]. When the silica NP surface is modified to be hydrophobic, they can absorb various proteins for *in vitro* delivery to manipulate cell functions. The Kane group demonstrated that hydrophobically functionalized silica NPs can deliver ribonuclease A and phosphor-Akt to human breast cancer cells (MCF-7) and rat neural stem cells, resulting in the initiation of cell death [115]. These results highlight the usefulness of silica NPs as protein delivery vehicle for the control of cell functions. Moreover, silica-coated liposomes were explored for the *in vivo* delivery of insulin to reduce glucose levels in a Wistar rat model [116]; the coated liposomes show enhanced stability and preserve insulin function. Interestingly, 50-nm silica NPs conjugated with insulin were recently found to direct rat mesenchymal stem cells to adipogenic differentiation *in vitro*, whereas unconjugated NPs have no effect on mesenchymal stem cell differentiation [117]. These discoveries may give rise to more applications of silica NPs as delivery vehicles in stem cell research.

Photodynamic therapy

Photodynamic therapy, a minimally invasive and minimally toxic alternative to chemo- and radiotherapy, is used clinically to treat a range of medical conditions, including malignant cancers. Most modern PDT applications involve three key components: a photosensitizer, a light source, and tissue oxygen. When activated by light of a specific wavelength, the photosensitizer transfers energy from its triplet excited state to a neighboring oxygen molecule to generate single oxygen ($^1O_2$) and other cytotoxic reactive oxygen species (ROS), which initiate the destruction of cells. For selective destruction of the target area, the photosensitizer can be applied locally to the target area, or photosensitive targets can be locally photoexcited. NPs offer a method to increase the aqueous solubility of the hydrophobic photosensitizers, their blood circulation, and their selective accumulation in tumor tissue, owing to the enhanced permeability and retention (EPR) effect. Silica NPs have recently emerged as promising vehicles for PDT owing to their high biocompatibility, controllable formation and physicochemical properties, as well as the possibility for tumor targeting through facile surface modification. The use of silica NPs for PDT specifically was recently reviewed by the Durand group [118]. Here, we will focus on using nonporous silica NPs for the delivery of photosensitizer.

The pioneering work on the encapsulation of photosensitizers in silica NPs was done by the Kopelman and Prasad groups in 2003. The former group embedded the photosensitizer *meta*-tetra(hydroxyphenyl)chlorin in silica NPs through a modified Stöber sol–gel process, during which (3-aminopropyl)triethoxysilane is introduced to strengthen the binding between the photosensitizer and the silica matrix [119]. The Prasad group entrapped the water-insoluble photosensitizing anticancer drug 2-devinyl-2-(1-hexyloxyethyl)pyropheophorbide in ultrafine organically modified 30-nm silica NPs and investigated their internalization by cancer cells and the destruction of the cells through photodynamic action (Fig. 7a–c).[30] Several other researcher groups extended this method to silica NPs of different structures and sizes as well as many other photosensitizers, including methylene blue, hypocrellin A, protoporphyrin IX, PC4, and *meta*-tetra(hydroxyphenyl)chlorin [99–101, 120–125]. Interestingly, the Prasad group fabricated silica NPs doped with a two-photon-absorbing fluorescent dye for two-photon PDT, a

promising technique for increasing tissue penetration of light to cure some internal diseases [120]. Recently, Li et al. used pH-responsive silica NPs for controllable $^1O_2$ generation [123]. The $^1O_2$ generation ability is much stronger in an acidic environment than in a basic one. Thus, these NPs provide a new promising strategy for targeting the acidic interstitial fluid of many kinds of tumors.

Photosensitizers have also been covalently conjugated to silica NPs to minimize leaching of the photosensitizers from the silica carrier before they reach the target site [102, 126–132]. In 2006, the Davydenko group covalently immobilized C_{60} on silica NPs for cancer PDT [127]. The Prasad group conjugated 2-devinyl-2-(1-hexyloxyethyl)pyropheophorbide with a silane group to covalently incorporate the photosensitizer inside the silica matrix (Fig. 7d–e) [102]. This strategy increased $^1O_2$ generation efficiency by about 1.7-fold [131].

In vivo evaluation is a critical step for clinical translation of silica NP–based PDT. He et al. developed phosphonate-terminated silica NPs encapsulating methylene blue using a water-in-oil microemulsion method [133]. The resulting particle platform is effective for simultaneous *in vivo* imaging and site-specific PDT with imaging guidance. When mice with HeLa tumors are treated with methylene blue–containing silica NPs and light irradiation, moderate efficacy is observed. Simon et al. demonstrated that protoporphyrin IX–containing silica NPs show better *in vivo* tumor accumulation in HCT 116, A549, and glioblastoma tumors in mice as compared to the free dye [100]. These silica NP based PDTs show the great promise for potential clinical application in cancer treatment. However, before they could be potentially clinically translated, much more preclinical evaluations are required to demonstrate the efficacy and selectivity as well as potential toxicity *in vivo*.

Silica NPs for gene delivery

Gene delivery is another major application of silica NPs besides the delivery of small molecules and proteins. The use of silica NPs for gene delivery has been explored because their surfaces can be easily modified with cationic molecules, which allow for the stable condensation with nucleotides that are highly negatively charged and the protection of them from nuclease in physiological condition. Additionally, silica is bio-inert and less toxic than some cationic polymers employed for gene delivery, and silica NPs are generally more stable than liposomes and other self-assembly nanostructures under physiological conditions. In the early 2000s, the Saltzeman group coupled silica NPs with a transfection reagent–DNA complex by simple co-incubation; the coupling enhances β-galactosidase gene expression by 750%, owing to the increased concentration of the complex at the cell surface [134–136]. However, Guo et al. reported that the percentage of cells that associate with DNA is not significantly influenced by the ternary complex, suggesting that the silica NPs are more than just a sedimentation agent; they may also act as a secondary transfection reagent [137]. These discoveries boosted the applications of silica NPs for gene delivery.

Condensation with surface-modified silica NPs

To the best of our knowledge, the Lehr group was the first to use surface-modified silica NPs for gene delivery [138, 139]. They modified the surface of silica NPs with amine groups and demonstrated that a modified silica NP–DNA complex can be used for transfection *in vitro*. Transfection efficiency can reach 30% of that of polyethylenimine when 100 μM chloroquine is added, and no toxicity is observed at the required concentration of modified silica NPs. Other researchers have reported cationic silica NPs with surface modified by amine groups [31, 47, 140–146], cationic macromolecules [147–150], or cations [151]. For example, the Csogor group studied the interactions of DNA with the silica NPs with different amino groups modified on surface and found that the NP with the shortest amine chain condenses the most DNAs [140]. The *in vitro* transfection capability of

amine-functionalized silica NPs was demonstrated by the Prasad group using organically modified silica NPs which condense plasmid encoding enhanced green fluorescent protein (GFP) (Fig. 8a–b) [142]. Peng et al. also used amino-silica NPs to deliver an antisense oligonucleotide to HeLa and A549 cells to inhibit cell proliferation [143]. The amino NPs show stronger inhibition and lower cytotoxicity than liposomes. In addition to nanospheres, amine groups decorated silica nanotubes can deliver GFP gene to COS-7 cells [47]. Due to the unique hollow structure of the nanotubes, the method can be extended to other cargo molecules, such as siRNA and proteins.

Coating the silica NP surface with cationic polymer is another way to facilitate the condensation with DNA. Zhu et al. reported that poly(L-lysine)-modified silica NPs bind and protect *c-myc* antisense oligonucleotides [147]. They noticed a decrease in cellular uptake efficiency and antisense effects on target genes in the presence of serum-containing medium. Further experiments showed that the oligonucleotide–silica NP complex interacts electrostatically with fetal calf serum proteins, and the interaction may result in the formation of complex–protein aggregates and hamper cellular uptake of the complex.

Other strategies

Most of the reported cationic silica NPs were prepared by initial formation of the silica NPs and subsequent surface modification with positively charged species. An alternative method involves the condensation of cationic polymers (e.g., polyethylenimine) with a silica source to form cationic silica NP hybrids in a one-pot reaction [150]. In addition to amino groups and cationic polymers, Ca^{2+} has been used to modify silica NPs, and the modified NPs can not only bind DNA but also target bone cells [151]. Viral collagen was also used to modify surface of silica colloidal crystals for DNA delivery [148].

Conventional gene-delivery vectors have been coupled with silica NPs to combine the advantages of multiple systems [149, 152, 153]. For example, the Kataoka group reported that silica-coated polyplexes loaded with plasmid DNA show enhanced transfection relative to uncoated polyplexes; the enhancement may be due to facilitated endosomal escape, possibly by protonation of the silica in acidic endosomal compartments [149]. Furthermore, the coated polyplexes also show reduced cytotoxicity. Silica NP–supported lipid bilayers have been reported for gene delivery as well; transfection efficiency depends on particle size and lipid composition [154]. Specifically, transfection efficiency decreases dramatically with increasing particle size: a 30-nm silica core shows the highest efficiency, whereas the efficiency of a 130-nm silica core is nearly zero. Smaller NPs may increase cellular internalization and speed up DNA release inside the cells.

Recently, there is much interest in the development of multifunctional or theranostic silica NPs, which can be used for both diagnostic imaging and gene therapy. For example, when doped with gadolinium oxide, surface-modified silica NPs can anchor DNA for therapeutic gene delivery and serve as contrast agents for magnetic resonance imaging (MRI) simultaneously [146].

In vivo evaluation

There have been only a few *in vivo* studies of silica NP–based gene delivery. Bharali et al. reported the first study using organically modified silica NPs as a nonviral vector for *in vivo* gene delivery and expression and the result is very encouraging (Fig. 8c–d) [31]. The efficiency of transfection through stereotaxic injection of a DNA–NP complex equals or exceeds that obtained with a viral vector. It was also demonstrated that this organically modified silica NP–mediated transfection can be used to manipulate the biology of neural stem cells or progenitor cells *in vivo* without damaging the cells. This landmark in nonviral

gene transfection reveals that organically modified silica NPs are highly promising not only for *in vivo* gene delivery but also for targeted brain-disease therapy. Choi et al. also reported that a complex between the granulocyte-macrophage colony-stimulating factor gene and silica NPs can correct acute leukopenia in dogs [144, 145].

More *in vivo* studies that fully explore the potential of silica NPs as targeted, highly efficient, and nontoxic gene-delivery vehicles are necessary. Other clinically relevant issues, such as scalability and shelf-life, also need to be addressed before such vehicles can be translated for clinical use. In one successful attempt to address such issues, Sameti et al. prepared lyophilizable cationic silica NPs for gene delivery by adding suitable lyoprotective agents [141]. Together, silica NP based gene therapy is highly promising for potential clinical applications.

Silica NPs for imaging and diagnosis

Nanotechnology offers unprecedented opportunities for addressing current challenges in cancer diagnosis and therapy. Nanoparticles carrying diagnostic probes can provide structural and metabolic information from disease sites. NP-based imaging techniques can markedly improve the detection and staging of cancers and their metastases. Besides the application for delivery of therapeutic agents, silica NPs are also actively employed as the platform for incorporating contrast reagents for molecular imaging. Owing to their versatility and robust chemistry, diagnostic probe–doped silica NPs can be easily adopted for molecular imaging techniques, including optical imaging (fluorescence and bioluminescence), MRI, radionuclide imaging (positron emission tomography (PET) and Single-photon emission computed tomography (SPECT)), computed tomography (CT), ultrasound, photoacoustic imaging, and Raman imaging. Single and multiple modal imaging techniques based on silica NPs have been actively explored during the past two decades, and many types of multifunctional silica NPs with applications for cancer diagnosis have been developed.

Optical imaging

The Blaaderen and Quellet groups were the first to incorporate organic fluorescent dyes into monodisperse silica NPs using the Stöber method [155, 156]. Subsequently, silica NPs doped with fluorescence dyes, QDs or rare-earth fluorescence NPs were extensively studied as optical imaging probes for various biological applications [157–161]. One of the most important applications is targeted cancer imaging both *in vitro* and *in vivo* [71, 75, 104, 162–183]. The Santra group prepared 70-nm fluorescein isothiocyanate–doped silica NPs by reverse microemulsion and then modified the NP surface with the trans-activating transcriptional activator peptide to enhance penetration of cell membranes and tissues [162]. The resulting NPs can efficiently label human lung adenocarcinoma (A549) cells. More interestingly, these NPs cross the blood-brain-barrier (BBB) when administered via the right common carotid artery, which supplies blood to the right side of the brain, in a Sprague–Dawley rat. This result indicates that diagnostic and therapeutic agents can be delivered to the brain using silica NPs without compromising the BBB. Choi et al. synthesized a new class of highly fluorescent core–shell silica NPs with narrow size distributions and enhanced photostability, and these NPs (called Cornell dots, or C dots) are widely applicable for a broad range of imaging techniques including intravital visualization of capillaries and macrophages, sentinel lymph node mapping, and peptide-mediated multicolor cell labeling for real-time imaging of tumor metastases and tracking of injected bone marrow cells in mice [166]. These results demonstrate that fluorescent core–shell silica NPs represent a powerful, novel imaging tool. Recently, the Mooney group reported the targeted imaging of ischemic tissues using dye-doped vascular endothelial growth factor-conjugated silica NPs

via the EPR effect in the murine hindlimb ischemic model, which opens new possibilities for treating large or multiple ischemic tissues [171].

Many fluorescent silica NPs are prepared by physical encapsulation of the dyes, which may leak from the silica matrix under physiological conditions. To eliminate such leakage, covalent conjugation methods have been adopted. For example, Mader et al. linked dyes to surface-modified silica NPs by means of azide-alkyne click chemistry [182]. Other groups and our group used a dye-silane precursor, with a stable chemical bond between the dye and silane group, to covalently link dyes to silica NPs with high stability [71, 104, 170].

Two-photon fluorescence imaging has several advantages over traditional one-photon fluorescence imaging for biomedical applications, including highly localized three-dimensional spatial excitation, lower photo-induced damage, longer observation time, less interference by autofluorescence, and deeper tissue penetration of light. Two-photon-absorbing dyes, such as 4,4'-diethylaminostyryl-2,2'-bipyridine Zn(II) [173], rare-earth dopants $NaYbF_4$:RE [180], and the fluorophore 4-[2-(4-diphenylamino-phenyl)-vinyl]-1-methyl-pyridinium iodide, have been incorporated into silica NPs for two-photon imaging [174]. Cellular-level two-photon fluorescence *ex vivo* imaging of whole-tumor mounts was demonstrated by the Belfield group using silica NPs doped with 2-(2,6-bis((*E*)-2-(7-(diphenylamino)-9,9-diethyl-9*H*-fluoren-2-yl)vinyl)-4*H*-pyran-4-ylidene)malononitrile [176]. Interestingly, $NaYbF_4$:RE upconversion fluorescence NPs emit tunable visible light (e.g., orange, yellow, green, cyan, blue, or pink) in response to near-infrared irradiation, and the color can be tuned simply by changing either the codopant concentration or the dopant species [175]. In addition to the two-photon fluorescence imaging, in order to increase the Stokes shift, He et al. recently presented a novel large Stokes shifting near-infrared (NIR) fluorescent silica NPs based on the principle of fluorescence resonance energy transfer [184]. Due to the small Stokes shit of many traditional NIR dyes, the interference and crosstalk between excitation light and the emitting signal could be a problem for *in vivo* applications. Two dyes, tris(2,2-bipyridyl)-dichlororuthenium(II) hexahydrate (RuBpy) and methylene blue (MB), were synchronously doped in silica NPs, resulting in the energy transfer from RuBpy to MB in the silica matrix and a near-infrared fluorescence emission with large Stokes shift (>200 nm).

QD–containing silica NPs are another class of fluorescent silica NPs [175, 177, 179, 185]. The Prasad group co-encapsulated quantum dots and magnetite NPs in organically modified silica NPs, which were then used for two-photon magnetically guided *in vitro* imaging [175]. The same group also reported silica NPs with encapsulated quantum rods for *in vitro* and *in vivo* imaging in tumor-bearing mice [179]. In addition, Le Guevel et al. reported a novel silica NP doped with fluorescent gold nanoclusters (<2 nm), which showed an emission in the near infrared region (670 nm) [178].

Magnetic resonance imaging

MRI is a widely used, noninvasive diagnostic technique with high spatial resolution (25–100 μm level) and excellent tissue contrast. Silica NPs encapsulating MRI contrast agents, including paramagnetic complexes (Ga^{3+}- or Mn^{2+}-based chelates) [186–188] and superparamagnetic iron oxide NPs [189–195], have been extensively studied. For example, a Ga^{3+}-containing silica NP reported by Ji et al. [195] and iron oxide NP–bearing silica NPs reported by Cho et al. [191] have been used for *in vivo* MRI. Recently, the Kim group loaded human mesenchymal stem cells with silica NPs that are dually labeled with a dye and magnetic NPs. The labeled cells were easy to be tracked in live NOD-SCID mice via optical imaging or MRI, permitting determination of the location and fate of the stem cells [192].

Positron emission tomography imaging

PET is a nuclear medicine imaging technique that detects pairs of gamma rays emitted indirectly by a positron-emitting radionuclide (tracer). Three-dimensional images of tracer concentration within the body are then reconstructed by computer analysis. PET is quantitative and highly sensitive, and there are no limitations on tissue penetration. However, it has relatively low spatial resolution and is associated with radiation risks and high cost. Radionuclides such as ^{64}Cu, ^{18}F, ^{68}Ga, and ^{124}I can be used as radioisotopes for PET. These radioisotopes have been incorporated into silica NPs for PET imaging application. For example, the Bolton and Hunter method has been used to label silica NPs with ^{124}I for PET imaging (Fig. 9a) [12, 196].

There is a clear trend toward hybrid imaging modalities in the molecular imaging field because no single modality meets all requirements in biomedical imaging, including high sensitivity, high resolution, low interference and low cost etc.. Developing multimodality imaging can offer synergistic advantages in providing much more diagnostic information than a singly modality. The robust silane chemistry and the easy formulation of silica NPs make them ideal entities for the construction of multi-modal imaging probes for *in vivo* applications [197, 198]. For example, the Prasad group synthesized multimodal organically modified silica NPs, conjugated with near-infrared fluorophores and further radiolabeled with ^{124}I for both optical and PET imaging *in vivo* [196]. Clearance and biodistribution were studied to demonstrate the potential of these biocompatible silica NPs as probes for *in vivo* imaging. Our group recently reported a convenient, one-pot synthesis of monodisperse, size-controlled silica nanoconjugate probes for dual-modal lymph node imaging of PET and NIR fluorescence [72]. We demonstrated that when the size of the silica nanoconjugates is controlled as small as 20 nm, they accumulate rapidly and effectively in lymph nodes, thus allowing for improved lymph node imaging *in vivo*. By further functionalizing the silica nanoconjugate surface with a DNA aptamer, AS1411, active targeting of lymphatic metastases was achieved. These dual labeled silica nanoconjugates hold great potential for improving the accuracy of clinical tumor staging by serving as probes for efficient noninvasive targeted imaging of metastatic lymph nodes.

As an illustration of the remarkable progress in the translation of targeted diagnostic silica NPs, C dots, reported by Wiesner and Bradbury groups, were recently approved by the US FDA for a first-in-human clinical trial (Fig. 9) [12]. These approximately 7-nm silica NPs encapsulate Cy5 dye and are surface functionalized with cyclic arginine-glycine-aspartic acid peptide ligands and radioiodine. They exhibit high-affinity, high-avidity binding, favorable tumor-to-blood ratios, efficient renal clearance, and enhanced tumor-selective accumulation in $\alpha_v\beta_3$ integrin–expressing melanoma xenografts in mice.

Other imaging techniques

Silica NPs have also been studied for other imaging techniques. For example, 1250-nm hollow silica microspheres with PEG modification on surface were reported as a novel contrast agent for *in vivo* ultrasound imaging of male rats after intratesticle injection [199, 200]. Silica NPs that encapsulate gold NPs or nanorods are useful for some other imaging applications. For example, Chen et al. reported recently that silica-coated gold nanorods produce a photoacoustic signal that is 3 times of the strength of that produced by uncoated nanorods; strong contrast enhancement in photoacoustic imaging was also demonstrated with this core–shell structure probe [201]. In addition, the Gambhir group recently reported gold– silica NPs functionalized with an epidermal growth factor receptor as multimodal contrast agents for Raman molecular imaging; this is the first example of Raman molecular imaging with core–shell NPs [202].

Safety and toxicity of silica NPs

The applications of silica NPs for therapy and diagnosis have already been demonstrated in many preclinical studies. To facilitate the potential clinical translation of these silica NPs, it is important to fully evaluate the safety and potential toxicity of these silica based nanomedicines. The toxicity and safety of various forms of silica was comprehensively reviewed by Napierska et al. [203] and Fruijtier-Polloth [204]. Until recently, toxicological research of silica particles focused mainly on "natural" crystalline silica particles with diameters of 0.5–10 μm, which are known to present an occupational inhalation exposure risk. Here, we will discuss the potential toxicity of amorphous, nanosized colloidal silica because of its biomedical applications as drug delivery vehicle and diagnostic probe as discussed above.

In vitro toxicity

Many *in vitro* evaluations of silica NP toxicity have been done [203, 205–207]. The toxicity of silica NPs depends strongly on physicochemical properties such as particle size, shape, porosity, chemical purity, surface chemistry, and solubility [208, 209]. Many researchers have observed that the cytotoxicity of silica NPs is size dependent [210–216]. For example, Gao and co-workers used human dermal fibroblasts to study the cellular uptake and cytotoxicity of monodisperse 80- and 500-nm silica NPs [212]. These investigators found that cell viability and mitochondrial membrane potential are more strongly affected by the smaller NPs than the larger NPs, but the adhesion and migration ability of the fibroblasts are impaired by NPs of both sizes. Passagne et al. also reported that 20 nm silica NPs are more toxic than 100 nm NPs; the cytotoxicity is associated to stress oxidative with up-production ROS and lipid peroxidation [216]. Oh et al. treated mouse alveolar macrophage (J774A.1) cells with hollow silica–titania NPs with uniform diameters of 25, 50, 75, 100, and 125 nm and found that cell viability, ROS production, and apoptosis and necrosis caused by the NPs are size dependent [210]. Among the various NPs investigated, 50-nm cationic NPs were found to be the most harmful to the macrophages.

The surface chemistry of silica NPs also plays an important role in their cytotoxicity [209, 210, 212, 217–219]. Morishige et al. compared interleukin-1b production levels in THP-1 human macrophage–like cells treated with 1000-nm silica NPs with or without surface functional groups (–COOH, $–NH_2$, $–SO_3H$, or –CHO) and found that all the surface modification dramatically suppresses interleukin-1b production by reducing ROS level [218].Brown et al. also reported that uncoated silica NPs induce an increased release of lactic acid dehydrogenase and interleukin-8, whereas surface modification with polyethylene glycol mitigates this effect [220]. Work performed by Chang et al. suggests that the cytotoxicity of silica NPs to various human cells can be substantially reduced by coating silica NPs with chitosan (which bears amino groups) [219]. However, Oh et al. found that amine-functionalized silica NPs with positively charged surfaces are more harmful to macrophage J774A.1 cells than silica NPs with anionic or neutral surface modification [210]. These contradictory results may be explained by the fact that the effects of the physicochemical properties of silica NPs on cytotoxicity are also cell-type dependent [219]. It is revealed that fibroblast cells with longer doubling times are more susceptible to injury induced by silica exposure than tumor cells with shorter doubling times.

The Ghandehari group has thoroughly evaluated the impacts of geometry, porosity, and surface charge of silica NPs on cellular toxicity and hemolytic activity (Fig. 10a, b). First, it was noted that there is a concentration threshold at ~100 μg/mL for the *in vitro* toxicity of silica NPs; below the threshold there is limited to no impact of the silica NPs of various physicochemical characteristics on membrane integrity, mitochondrial function, phagocytosis or cell death [221]. They observed that surface charge and porosity of the NPs

are the major factors that influenced the cellular association and cytotoxicity of the silica NPs. Positively charged NPs are more toxic than the negatively charged ones [209, 217]. Nonporous silica NPs are markedly less toxic than mesoporous silica NPs [209]. Geometry does not influence the extent of cellular association nor the cytotoxicity in the study, which compares mesoporous silica nanorods with aspect ratio of 2, 4, and 8 [209, 221]. Cell type also plays an important role in determining the *in vitro* toxicity; cancer epithelial cells are highly resistant to the silica NP treatment, while the toxicity on macrophages is predominantly surface-charge-dependent [209, 217]. This group as well as Lin group also investigated the blood biocompatibility of the silica NPs and found that the hemolytic activity was porosity and geometry dependent for bare silica NPs, and surface charge dependent for amine-modified silica NPs [209, 222].

In another recent study, Rabolli et al. investigated the influence of silica NP size, surface area, and microporosity on *in vitro* cytotoxic activity in four cell types (macrophages, fibroblasts, endothelial cells, and erythrocytes) [223]. The physicochemical parameter that governs the response to the NPs varies by cell types: in murine macrophages, the cytotoxic response increases with external surface area and decreases with micropore volume; in human endothelial cells and mouse embryo fibroblasts, cytotoxicity increases with increasing surface roughness and decreasing diameter; in human erythrocytes, hemolytic activity increases with particle diameter.

Researchers have also tried to underline the mechanisms of silica NP cytotoxicity. Liu et al. reported that silica NPs markedly induce ROS production, mitochondrial depolarization, and apoptosis in human umbilical vein endothelial cells [224]. These investigators demonstrated that silica NPs induce dysfunction of endothelial cells through oxidative stress via the JNK, p53, and NF-kB pathways. Ye et al. reported similar results with the L-02 line of human hepatic cells [225]. The Ghandehari group also noted that the cytotoxicity may be associated with the autophagic processes in cellular coping mechanisms for silica NPs [221].

Although several *in vitro* studies of silica NPs indicate that they are cytotoxic, other studies have found that they show low or no toxicity *in vitro* [217]. In fact, Brunner et al. used amorphous silica NPs as a nontoxic control in their studies [226]. Using the Comet assay, Barnes et al. found no significant genotoxicity for the tested silica NPs on 3T3-L1 fibroblasts after incubation for 3, 6, and 24 h [227]. The results were independently validated in two separate laboratories.

The determinants of the observed toxicity seem to be complicated and vary with the type of silica NPs and the cells. Unfortunately, in many published studies, the silica NPs were not characterized adequately enough to allow us to draw conclusions about whether the observed cytotoxicity necessarily implies that silica NPs are generally hazardous. More-careful *in vitro* studies with well-characterized silica NPs are necessary for clarification of their cytotoxicity; more mechanistic studies of such cytotoxicity are also highly desired.

In vivo toxicity

Although many *in vivo* studies of the pulmonary toxicity of inhaled silica NPs have been performed, the systemic toxicity of intravenously administered silica NPs has not been extensively investigated [62, 196, 208, 228–238]. Tang and co-workers recently reported that mesoporous hollow silica NPs show low and dose-dependent toxicity when intravenously injected at single or repeated doses [234]. For a single dose, the median lethal dose (LD_{50}) of 110-nm NPs exceeded 1000 mg/kg. For repeated doses, no deaths were observed after mice were exposed to NPs at 20, 40, and 80 mg/kg by continuous intravenous administration for 14 days. The intravenously injected NPs accumulate mainly in mononuclear phagocytic cells in the liver and spleen, and the total clearance time of the

particles is estimated to exceed 4 weeks. Additionally, Cho et al. observed size-dependent tissue distribution and elimination of 50-, 100-, and 200-nm nonporous silica NPs administered by a single intravenous injection [228]. The incidence and severity of an inflammatory response increases transiently within 12 h post the injection of 200- or 100-nm silica NPs, but injection of 50-nm particles elicits no significant response. Similarly, these investigators found that the silica NPs are trapped by macrophages in the spleen and liver and remain there until 4 weeks after a single injection. In contrast, Nishimori et al. found that smaller NPs are more toxic than larger NPs [231, 236]. Their studies revealed that 70-nm NPs induce liver injury at 30 mg/kg dose, whereas 300- or 1000-nm NPs have no effect even at 100 mg/kg. Further investigation of the effect of particle size on the systemic toxicity of well-characterized NPs is necessary.

Interestingly, Souris et al. discovered that the surface charge of silica NPs also plays an important role in hepatobiliary excretion [230]. Positively charged silica NPs are quickly excreted from the liver into the gastrointestinal tract, whereas negatively charged NPs remain sequestered in the liver. These investigators suggested that charge-dependent adsorption of serum proteins greatly facilitate the hepatobiliary excretion. The Ghandehari group evaluated the *in vivo* toxicity of silica NPs in immune-competent mice when administered intravenously and found that *in vivo* toxicity of silica NPs was mainly influenced by the porosity and surface charge (Fig. 10c) [208, 239]. Nonporous silica NPs of 120 nm exhibit low systemic toxicity with the highest maximum tolerated dose (MTD) of 450 mg/kg; mesoporous silica NPs of 120 nm have considerable systemic toxicity with MTDs ranging from 30 to 65 mg/kg. However, the toxicity was attenuated when mesoporous silica NPs were modified with primary amine groups (MTD = 100–150 mg/kg). Interestingly, they noted that the geometrical features have no effect on the *in vivo* toxicity of silica NPs. In contrast, the shape of silica NPs was found to dramatically affect their toxicity toward developing vertebrate embryos, as was reported by Nelson et al., who used the embryonic zebrafish as a model system in their studies [237]. These investigators showed that silica nanomaterials with aspect ratios >1 are highly toxic (LD_{50} = 110 pg/g embryo) and cause embryo deformities, whereas silica nanomaterials with an aspect ratio of 1 are neither toxic nor teratogenic at the same concentrations.

Silica NPs may be neurotoxic. Sun and co-workers recently reported that silica NPs may negatively affect the striatum and dopaminergic neurons in rats, in addition to being a potential risk factor for neurodegenerative diseases [232]. The results indicated that upon intranasal instillation, silica NPs enter the brain and are deposited predominantly in the striatum; the exposure to silica NPs induces oxidative damage and increased inflammatory response in the striatum. In contrast, Barandeh et al. reported the opposite result in a recently published study, in which Drosophila were fed orally with organically modified silica NP solution of different concentrations [240]. They showed that these silica NPs are biocompatible toward living neuronal tissues and living organisms with minimal effects on normal cellular functions. Silica NPs internalized in living neuronal cells do not activate aberrant neuronal death pathways, or affect the long distance transport pathway (axonal transport), which is essential for the growth, maintenance and survival of all neurons. It is noticeable that the silica NPs were administered through very different routes and animal models are different in these two studies, which could be the reason that drastically different results were observed. Future investigations of the neurotoxic of silica NPs of different properties in more animal models are highly desired.

Silica NPs may have more prominent effect on pregnant animals. The Tsutsumi group reported that 70- and 35-nm silica NPs can cause pregnancy complications when injected intravenously into pregnant mice, suggesting that the NPs cross the placenta barrier in pregnant mice [233]. In addition, mice treated with these NPs have smaller uteri and smaller

fetuses than untreated controls. Interestingly, larger silica NPs (300 and 1000 nm) do not induce these complications.

Several groups have reported that silica NPs or implants can degrade reasonably fast *in vivo* [78, 106, 241] and silica NPs can be cleared from body over time [62, 196], which suggests that the long-term *in vivo* toxicity of silica NPs could be low. Because silica is generally considered to be inert, it is commonly used to coat other NPs, such as gold NPs and iron oxide NPs. The toxicity of silica-coated core–shell NPs has been studied by several researchers [229, 235]. For example, after intravenous administration of silica-coated gold NPs, a mild inflammatory response and an increase in oxidative stress are observed in the liver; both effect subside by 2 weeks after administration [235]. Kim et al. demonstrated that 50-nm silica-coated magnetic NPs cause no apparent toxicity after intraperitoneal administration [229]. Nevertheless, because silica NPs are promising nanomaterials for biomedical applications, the biocompatibility and long-term safety and clearance of well-characterized silica NPs must be more carefully evaluated in preclinical studies before they could be translated for clinical use.

Conclusions and future perspectives

Silica NPs offer a promising alternative to organic drug delivery systems and exhibit many unique properties, such as highly controllable size and shape. Nonporous silica NPs have found numerous biomedical applications for the delivery of drugs, proteins, and genes and for molecular imaging. However, before silica NPs can be used routinely in clinic, some major challenges must be overcome, including the need for improved drug loading (high drug loading and high incorporation efficiency), spatial and temporal control of drug release, highly efficient targeting of disease sites, scalable manufacturing, long-term stability, and well-understood biocompatibility and potential toxicity. Organo-silica hybrid NPs, which are expected to have both the unique properties of silica NPs and the functionalities (e.g., photoresponsiveness) introduced by organic functional groups, could provide more-sophisticated silica based nanomedicines with highly controllable drug loading and responsive drug release [102, 103, 242–248]. To achieve highly specific targeting of diseases, correlation between the physicochemical properties of silica NPs and their behavior in biological systems must be fully elucidated. Furthermore, the possibility of directing silica NPs specifically to disease sites by means of targeting ligands, such as antibodies and aptamers, also needs to be further explored. A complete understanding of the toxicity profile and potential environmental impact of silica NPs will require tremendous effort on the part of toxicologists, pathologists, biologists, environmentalists, and material scientists. Because nanomedicines are typically more heterogeneous than well-defined small-molecule drugs, this task may be nontrivial. However, a thorough understanding of the toxicity profile is not only of great scientific interest but also a prerequisite for clinical application of silica NPs. Nevertheless, we anticipate that new synthetic methods and smart designs based on silica NPs will provide solutions to all the above-mentioned issues and will eventually lead to the development of powerful nanomedicines for early diagnosis and specific personalized therapy of many diseases.

Acknowledgments

J.C. acknowledges supports from the NIH (Director’s New Innovator Award program 1DP2OD007246-01 and 1R21CA152627). L.T. was funded at University of Illinois at Urbana-Champaign from NIH National Cancer Institute Alliance for Nanotechnology in Cancer ‘Midwest Cancer Nanotechnology Training Centre’ Grant R25 CA154015A. We thank Ms. Catherine Yao for her help on drawing the 3D images.

References

1. Peer D, Karp JM, Hong S, Farokhzad OC, Margalit R, Langer R. Nat. Nanotechnol. 2007; 2:751–760. [PubMed: 18654426]
2. Jain RK, Stylianopoulos T. Nat. Rev. Clin. Oncol. 2010; 7:653–664. [PubMed: 20838415]
3. Petros RA, DeSimone JM. Nat. Rev. Drug Discov. 2010; 9:615–627. [PubMed: 20616808]
4. Duncan R. Nat. Rev. Cancer. 2006; 6:688–701. [PubMed: 16900224]
5. Davis ME, Chen Z, Shin DM. Nat. Rev. Drug Discov. 2008; 7:771–782. [PubMed: 18758474]
6. Ferrari M. Nat. Rev. Cancer. 2005; 5:161–171. [PubMed: 15738981]
7. Zhang L, Gu FX, Chan JM, Wang AZ, Langer RS, Farokhzad OC. Clin. Pharmacol. Ther. 2008; 83:761–769. [PubMed: 17957183]
8. Kim BYS, Rutka JT, Chan WCW. N. Engl. J. Med. 2010; 363:2434–2443. [PubMed: 21158659]
9. O'Brien MER, Wigler N, Inbar M, Rosso R, Grischke E, Santoro A, Catane R, Kieback DG, Tomczak P, Ackland SP, Orlandi F, Mellars L, Alland L, Tendler C. Annals. of Oncology. 2004; 15:440–449. [PubMed: 14998846]
10. Slowing II, Vivero-Escoto JL, Wu CW, Lin VSY. Adv. Drug Deliv. Rev. 2008; 60:1278–1288. [PubMed: 18514969]
11. Barbe C, Bartlett J, Kong LG, Finnie K, Lin HQ, Larkin M, Calleja S, Bush A, Calleja G. Adv. Mater. 2004; 16:1959–1966.
12. Benezra M, Penate-Medina O, Zanzonico PB, Schaer D, Ow H, Burns A, DeStanchina E, Longo V, Herz E, Iyer S, Wolchok J, Larson SM, Wiesner U, Bradbury MS. J. Clin. Invest. 2011; 121:2768–2780. [PubMed: 21670497]
13. Bradbury MS, Phillips E, Montero PH, Cheal SM, Stambuk H, Durack JC, Sofocleous CT, Meester RJC, Wiesner U, Patel S. Integrative Biology. 2013; 5:74–86. [PubMed: 23138852]
14. Vallet-Regi M, Balas F, Arcos D, Chem Angew. Int. Ed. 2007; 46:7548–7558.
15. Trewyn BG, Slowing II, Giri S, Chen HT, Lin VSY. Acc. Chem. Res. 2007; 40:846–853. [PubMed: 17645305]
16. Pasqua L, Cundari S, Ceresa C, Cavaletti G. Curr. Med. Chem. 2009; 16:3054–3063. [PubMed: 19689282]
17. Vivero-Escoto JL, Slowing II, Trewyn BG, Lin VSY. Small. 2010; 6:1952–1967. [PubMed: 20690133]
18. Piao Y, Burns A, Kim J, Wiesner U, Hyeon T. Adv. Funct. Mater. 2008; 18:3745–3758.
19. Stober W, Fink A, Bohn E. J. Colloid Interface Sci. 1968; 26:62–69.
20. Bogush GH, Tracy MA, Zukoski Iv CF. J. Non-Cryst. Solids. 1988; 104:95–106.
21. Van Blaaderen A, Van Geest J, Vrij A. J. Colloid Interface Sci. 1992; 154:481–501.
22. Herbert G. J. Eur. Ceram. Soc. 1994; 14:205–214.
23. Kim JW, Kim LU, Kim CK. Biomacromolecules. 2007; 8:215–222. [PubMed: 17206810]
24. Nozawa K, Gailhanou H, Raison L, Panizza P, Ushiki H, Sellier E, Delville JP, Delville MH. Langmuir. 2005; 21:1516–1523. [PubMed: 15697302]
25. Hartlen KD, Athanasopoulos APT, Kitaev V. Langmuir. 2008; 24:1714–1720. [PubMed: 18225928]
26. Yokoi T, Wakabayashi J, Otsuka Y, Fan W, Iwama M, Watanabe R, Aramaki K, Shimojima A, Tatsumi T, Okubo T. Chem. Mater. 2009; 21:3719–3729.
27. Yokoi T, Sakamoto Y, Terasaki O, Kubota Y, Okubo T, Tatsumi T. J. Am. Chem. Soc. 2006; 128:13664–13665. [PubMed: 17044675]
28. Lee YG, Park JH, Oh C, Oh SG, Kim YC. Langmuir. 2007; 23:10875–10878. [PubMed: 17902722]
29. Meng Z, Xue CY, Zhang QH, Yu XH, Xi K, Jia XD. Langmuir. 2009; 25:7879–7883. [PubMed: 19358595]
30. Roy I, Ohulchanskyy TY, Pudavar HE, Bergey EJ, Oseroff AR, Morgan J, Dougherty TJ, Prasad PN. J. Am. Chem. Soc. 2003; 125:7860–7865. [PubMed: 12823004]

31. Bharali DJ, Klejbor I, Stachowiak EK, Dutta P, Roy I, Kaur N, Bergey EJ, Prasad PN, Stachowiak MK. Proc. Natl. Acad. Sci. 2005; 102:11539–11544. [PubMed: 16051701]
32. Vanhelden AK, Jansen JW, Vrij A. J. Colloid Interface Sci. 1981; 81:354–368.
33. Osseoasare K, Arriagada FJ. Colloids Surf. 1990; 50:321–339.
34. Arriagada FJ, Osseoasare K. Colloids Surf. 1992; 69:105–115.
35. Arriagada, FJ.; Osseoasare, K. The Colloid Chemistry of Silica. Bergna, HE., editor. Washington, DC: American Chemical Society; 1994. p. 113-128.
36. Arriagada FJ, Osseo-Asare K. Colloids Surf A. 1999; 154:311–326.
37. Arriagada FJ, Osseo-Asare K. J. Colloid Interface Sci. 1999; 211:210–220. [PubMed: 10049537]
38. Osseo-Asare K, Arriagada FJ. J. Colloid Interface Sci. 1999; 218:68–76. [PubMed: 10489280]
39. Finnie KS, Bartlett JR, Barbé CJA, Kong L. Langmuir. 2007; 23:3017–3024. [PubMed: 17300209]
40. Bagwe RP, Yang CY, Hilliard LR, Tan WH. Langmuir. 2004; 20:8336–8342. [PubMed: 15350111]
41. Jin YH, Lohstreter S, Pierce DT, Parisien J, Wu M, Hall C, Zhao JXJ. Chem. Mater. 2008; 20:4411–4419.
42. Guerrero-Martinez A, Perez-Juste J, Liz-Marzan LM. Adv. Mater. 2010; 22:1182–1195. [PubMed: 20437506]
43. Geng Y, Dalhaimer P, Cai SS, Tsai R, Tewari M, Minko T, Discher DE. Nat. Nanotechnol. 2007; 2:249–255. [PubMed: 18654271]
44. Chauhan VP, Popović Z, Chen O, Cui J, Fukumura D, Bawendi MG, Jain RK. Chem Angew Int. Ed. 2011; 50:11417–11420.
45. Kwon NH, Beaux MF, Ebert C, Wang L, Lassiter BE, Park YH, McIiroy DN, Hovde CJ, Bohach GA. Nano Lett. 2007; 7:2718–2723. [PubMed: 17655369]
46. Son SJ, Bai X, Nan A, Ghandehari H, Lee SB. J. Controlled Release. 2006; 114:143–152.
47. Chen CC, Liu YC, Wu CH, Yeh CC, Su MT, Wu YC. Adv. Mater. 2005; 17 404−+
48. Müllner M, Yuan J, Weiss S, Walther A, Förtsch M, Drechsler M, Müller AHE. J. Am. Chem. Soc. 2010; 132:16587–16592. [PubMed: 21028813]
49. Kuijk A, van Blaaderen A, Imhof A. J. Am. Chem. Soc. 2011; 133:2346–2349. [PubMed: 21250633]
50. Gao C, Lu Z, Yin Y. Langmuir. 2011; 27:12201–12208. [PubMed: 21861481]
51. Deng ZW, Zhen ZP, Hu XX, Wu SL, Xu ZS, Chu PK. Biomaterials. 2011; 32:4976–4986. [PubMed: 21486679]
52. Liu HY, Chen D, Li LL, Liu TL, Tan LF, Wu XL, Tang FQ. Chem Angew Int. Ed. 2011; 50:891–895.
53. Yan EY, Fu YL, Wang X, Ding Y, Qian HQ, Wang CH, Hu Y, Jiang XQ. J. Mater. Chem. 2011; 21:3147–3155.
54. Li LL, Tang FQ, Liu HY, Liu TL, Hao NJ, Chen D, Teng X, He JQ. ACS Nano. 2010; 4:6874–6882. [PubMed: 20973487]
55. Fujiwara M, Shiokawa K, Hayashi K, Morigaki K, Nakahara Y. J. Biomed. Mater. Res. 2007; 81A: 103–112.
56. Albanese A, Tang PS, Chan WCW. Annu. Rev. Biomed. Eng. 2012; 14:1–16. [PubMed: 22524388]
57. Verma A, Uzun O, Hu YH, Hu Y, Han HS, Watson N, Chen SL, Irvine DJ, Stellacci F. Nat. Mater. 2008; 7:588–595. [PubMed: 18500347]
58. Kim B, Han G, Toley BJ, Kim CK, Rotello VM, Forbes NS. Nat. Nanotechnol. 2010; 5:465–472. [PubMed: 20383126]
59. Bagwe RP, Hilliard LR, Tan W. Langmuir. 2006; 22:4357–4362. [PubMed: 16618187]
60. Estephan ZG, Jaber JA, Schlenoff JB. Langmuir. 2010; 26:16884–16889. [PubMed: 20942453]
61. Legrand S, Catheline A, Kind L, Constable EC, Housecroft CE, Landmann L, Banse P, Pielesa U, Wirth-Heller A. New J. Chem. 2008; 32:588–593.
62. He XX, Nie HL, Wang KM, Tan WH, Wu X, Zhang PF. Anal. Chem. 2008; 80:9597–9603. [PubMed: 19007246]

63. Nakamura M, Ishimura K. Langmuir. 2008; 24:12228–12234. [PubMed: 18823130]
64. He Q, Zhang J, Shi J, Zhu Z, Zhang L, Bu W, Guo L, Chen Y. Biomaterials. 2010; 31:1085–1092. [PubMed: 19880176]
65. Yague C, Moros M, Grazu V, Arruebo M, Santamaria J. Chem. Eng. J. 2008; 137:45–53.
66. Rio-Echevarria IM, Selvestrel F, Segat D, Guarino G, Tavano R, Causin V, Reddi E, Papini E, Mancin F. J. Mater. Chem. 2010; 20:2780–2787.
67. Thierry B, Zimmer L, McNiven S, Finnie K, Barbé C, Griesser HJ. Langmuir. 2008; 24:8143–8150. [PubMed: 18590299]
68. Ohno K, Akashi T, Tsujii Y, Yamamoto M, Tabata Y. Biomacromolecules. 2012; 13:927–936. [PubMed: 22324307]
69. Jia G, Cao Z, Xue H, Xu Y, Jiang S. Langmuir. 2009; 25:3196–3199. [PubMed: 19437722]
70. Radhakrishnan B, Ranjan R, Brittain WJ. Soft Matter. 2006; 2:386–396.
71. Kumar R, Roy I, Hulchanskyy TY, Goswami LN, Bonoiu AC, Bergey EJ, Tramposch KM, Maitra A, Prasad PN. ACS Nano. 2008; 2:449–456. [PubMed: 19206569]
72. Tang L, Yang X, Dobrucki LW, Chaudhury I, Yin Q, Yao C, Lezmi S, Helferich WG, Fan TM, Cheng J. Chem Angew Int. Ed. 2012; 51:12721–12726.
73. Yang L, Zhang XB, Ye M, Jiang JH, Yang RH, Fu T, Chen Y, Wang KM, Liu C, Tan WH. Adv. Drug Deliv. Rev. 2011; 63:1361–1370. [PubMed: 22016112]
74. Medley CD, Bamrungsap S, Tan WH, Smith JE. Anal. Chem. 2011; 83:727–734. [PubMed: 21218774]
75. Cai L, Chen ZZ, Chen MY, Tang HW, Pang DW. Biomaterials. 2013; 34:371–381. [PubMed: 23084552]
76. Unger K, Rupprecht H, Valentin B, Kircher W. Drug Dev. Ind. Pharm. 1983; 9:69–91.
77. Quintanar-Guerrero D, Ganem-Quintanar A, Nava-Arzaluz MG, Pinon-Segundo E. Expert Opin. Drug Deliv. 2000; 6:485–498. [PubMed: 19413456]
78. Kortesuo P, Ahola M, Karlsson S, Kangasniemi I, Yli-Urpo A, Kiesvaara J. Biomaterials. 2000; 21:193–198. [PubMed: 10632401]
79. Radin S, El-Bassyouni G, Vresilovic EJ, Schepers E, Ducheyne P. Biomaterials. 2005; 26:1043–1052. [PubMed: 15369693]
80. Galagudza MM, Korolev DV, Sonin DL, Postnov VN, Papayan GV, Uskov IS, Belozertseva AV, Shlyakhto EV. Int. J. Nanomedicine. 2007; 5:231–237. [PubMed: 20463939]
81. Borak B, Arkowski J, Skrzypiec M, Ziolkowski P, Krajewska B, Wawrzynska M, Grotthus B, Gliniak H, Szelag A, Mazurek W, Bialy D, Maruszewski K. Biomed. Mater. 2007; 2:220–223. [PubMed: 18458478]
82. Lopez T, Bata-Garcia JL, Esquivel D, Ortiz-Islas E, Gonzalez R, Ascencio J, Quintana P, Oskam G, Alvarez-Cervera FJ, Heredia-Lopez FJ, Gongora-Alfaro JL. Int. J. Nanomedicine. 2011; 6:19–31. [PubMed: 21289978]
83. Li ZZ, Xu SA, Wen LX, Liu F, Liu AQ, Wang Q, Sun HY, Yu W, Chen JF. J. Controlled Release. 2006; 111:81–88.
84. Yang J, Lee J, Kang J, Lee K, Suh JS, Yoon HG, Huh YM, Haam S. Langmuir. 2008; 24:3417–3421. [PubMed: 18324841]
85. Lay CL, Liu HQ, Wu DC, Liu Y. Chem.-Eur. J. 2010; 16:3001–3004. [PubMed: 20151441]
86. Cao AN, Ye ZM, Cai ZW, Dong EY, Yang XW, Liu GB, Deng XY, Wang YL, Yang ST, Wang HF, Wu MH, Liu YF, Chem Angew. Int. Ed. 2010; 49:3022–3025.
87. Ma D, Li M, Patil AJ, Mann S. Adv. Mater. 2004; 16:1838–1841.
88. Kortesuo P, Ahola M, Kangas M, Yli-Urpo A, Kiesvaara J, Marvola M. Int. J. Pharm. 2001; 221:107–114. [PubMed: 11397572]
89. Kortesuo P, Ahola M, Kangas M, Leino T, Laakso S, Vuorilehto L, Yli-Urpo A, Kiesvaara J, Marvola M. J. Controlled Release. 2001; 76:227–238.
90. Inama L, Diré S, Carturan G, Cavazza A. J. Biotechnol. 1993; 30:197–210. [PubMed: 7764074]
91. Santos EM, Radin S, Ducheyne P. Biomaterials. 1999; 20:1695–1700. [PubMed: 10503970]
92. Böttcher H, Slowik P, Süβ W. J. Sol-Gel Sci. Technol. 1998; 13:277–281.

93. Radin S, Ducheyne P, Kamplain T, Tan BH. J. Biomed. Mater. Res. 2001; 57:313–320. [PubMed: 11484196]
94. Albarran L, Lopez T, Quintana P, Chagoya V. Colloids Surf., A. 2011; 384:131–136.
95. He XX, Hai L, Su J, Wang KM, Wu X. Nanoscale. 2011; 3:2936–2942. [PubMed: 21623439]
96. Stevens EV, Carpenter AW, Shin JH, Liu JS, Der CJ, Schoenfisch MH. Mol. Pharm. 2010; 7:775–785. [PubMed: 20205473]
97. Georgelin T, Bombard S, Siaugue JM, Cabuil V. Chem Angew Int. Ed. 2010; 49:8897–8901.
98. Shin JH, Metzger SK, Schoenfisch MH. J. Am. Chem. Soc. 2007; 129:4612–4619. [PubMed: 17375919]
99. Gupta A, Goswami LN, Ethirajan M, Missert J, Rao KVR, Ohulchanskyy T, Roy I, Morgan J, Prasad PN, Pandey RK. J. Porphyrins Phthalocyanines. 2011; 15:401–411.
100. Simon V, Devaux C, Darmon A, Donnet T, Thiénot E, Germain M, Honnorat J, Duval A, Pottier A, Borghi E, Levy L, Marill J. Photochem. Photobiol. 2010; 86:213–222. [PubMed: 19769577]
101. Compagnin C, Bau L, Mognato M, Celotti L, Miotto G, Arduini M, Moret F, Fede C, Selvestrel F, Echevarria IMR, Mancin F, Reddi E. Nanotechnology. 2009; 20
102. Ohulchanskyy TY, Roy I, Goswami LN, Chen Y, Bergey EJ, Pandey RK, Oseroff AR, Prasad PN. Nano Lett. 2007; 7:2835–2842. [PubMed: 17718587]
103. Della Rocca J, Huxford RC, Comstock-Duggan E, Lin W. Chem Angew Int. Ed. 2011; 50:10330–10334.
104. Tang L, Fan TM, Borst LB, Cheng J. ACS Nano. 2012; 6:3954–3966. [PubMed: 22494403]
105. Tang L, Gabrielson NP, Uckun FM, Fan TM, Cheng J. Mol. Pharm. 2013; 10:883–892. [PubMed: 23301497]
106. Finnie K, Waller D, Perret F, Krause-Heuer A, Lin H, Hanna J, Barbé C. J. Sol-Gel Sci. Technol. 2009; 49:12–18.
107. Li LL, Guan YQ, Liu HY, Hao NJ, Liu TL, Meng XW, Fu CH, Li YZ, Qu QL, Zhang YG, Ji SY, Chen L, Chen D, Tang FQ. ACS Nano. 2011; 5:7462–7470. [PubMed: 21854047]
108. Hu Y, Zheng XT, Chen JS, Zhou MJ, Li CM, Lou XW. J. Mater. Chem. 2011; 21:8052–8056.
109. Hu KW, Hsu KC, Yeh CS. Biomaterials. 2010; 31:6843–6848. [PubMed: 20542331]
110. Chi FL, Guo YN, Liu J, Liu YL, Huo QS. J. Phys. Chem. C. 2010; 114:2519–2523.
111. Huo QS, Liu J, Wang LQ, Jiang YB, Lambert TN, Fang E. J. Am. Chem. Soc. 2006; 128:6447–6453. [PubMed: 16683810]
112. Tan A, Simovic S, Davey AK, Rades T, Prestidge CA. J. Controlled Release. 2009; 134:62–70.
113. Ellerby L, Nishida C, Nishida F, Yamanaka S, Dunn B, Valentine J, Zink J. Science. 1992; 255:1113–1115. [PubMed: 1312257]
114. Betancor L, Luckarift HR. Trends Biotechnol. 2010; 26:566–572. [PubMed: 18757108]
115. Bale SS, Kwon SJ, Shah DA, Banerjee A, Dordick JS, Kane RS. ACS Nano. 2010; 4:1493–1500. [PubMed: 20201555]
116. Dwivedi N, Arunagirinathan MA, Sharma S, Bellare J. J. Nanomater. 2010; 2010 ID 652048.
117. Liu D, He XX, Wang KM, He CM, Shi H, Jian LX. Bioconjug. Chem. 2010; 21:1673–1684. [PubMed: 20735012]
118. Couleaud P, Morosini V, Frochot C, Richeter S, Raehm L, Durand JO. Nanoscale. 2010; 2:1083–1095. [PubMed: 20648332]
119. Yan F, Kopelman R. Photochem. Photobiol. 2003; 78:587–591. [PubMed: 14743867]
120. Kim S, Ohulchanskyy TY, Pudavar HE, Pandey RK, Prasad PN. J. Am. Chem. Soc. 2007; 129:2669–2675. [PubMed: 17288423]
121. Zhou JH, Zhou L, Dong C, Feng YY, Wei SH, Shen J, Wang XS. Mater. Lett. 2008; 62:2910–2913.
122. Zhao B, Yin J-J, Bilski PJ, Chignell CF, Roberts JE, He Y-Y. Toxicol. Appl. Pharmacol. 2009; 241:163–172. [PubMed: 19695274]
123. Li ZB, Wang JG, Chen JR, Lei WH, Wang XS, Zhang BW. Nanotechnology. 2010; 21:115102. [PubMed: 20173245]

124. Zhou L, Liu JH, Zhang J, Wei SH, Feng YY, Zhou JH, Yu BY, Shen J. Int. J. Pharm. 2010; 386:131–137. [PubMed: 19922781]
125. Qian J, Wang D, Cai FH, Zhan QQ, Wang YL, He SL. Biomaterials. 2012; 33:4851–4860. [PubMed: 22484045]
126. Cheng S-H, Lee C-H, Yang C-S, Tseng F-G, Mou C-Y, Lo L-W. J. Mater. Chem. 2009; 19:1252–1257.
127. Davydenko MO, Radchenko EO, Yashchuk VM, Dmitruk IM, Prylutskyy YI, Matishevska OP, Golub AA. J. Mol. Liq. 2006; 127:145–147.
128. Rossi LM, Silva PR, Vono LLR, Fernandes AU, Tada DB, Baptista MS. Langmuir. 2008; 24:12534–12538. [PubMed: 18834155]
129. Tu H-L, Lin Y-S, Lin H-Y, Hung Y, Lo L-W, Chen Y-F, Mou C-Y. Adv. Mater. 2009; 21:172–177.
130. Guo YY, Rogelj S, Zhang P. Nanotechnology. 2010; 21 065102.
131. Kim S, Ohulchanskyy TY, Bharali D, Chen YH, Pandey RK, Prasad PN. J. Phys. Chem. C. 2009; 113:12641–12644.
132. Huang P, Li ZM, Lin J, Yang DP, Gao G, Xu C, Bao L, Zhang CL, Wang K, Song H, Hu HY, Cui DX. Biomaterials. 2011; 32:3447–3458. [PubMed: 21303717]
133. He XX, Wu X, Wang KM, Shi BH, Hai L. Biomaterials. 2009; 30:5601–5609. [PubMed: 19595455]
134. Luo D, Saltzman WM. Nat. Biotechnol. 2000; 18:893–895. [PubMed: 10932162]
135. Luo D, Han E, Belcheva N, Saltzman WM. J. Controlled Release. 2004; 95:333–341.
136. Gemeinhart RA, Luo D, Saltzman WM. Biotechnol. Prog. 2005; 21:532–537. [PubMed: 15801794]
137. Guo C, Gemeinhart RA. Mol. Pharm. 2004; 1:309–316. [PubMed: 15981590]
138. Kneuer C, Sameti M, Bakowsky U, Schiestel T, Schirra H, Schmidt H, Lehr CM. Bioconjug. Chem. 2000; 11:926–932. [PubMed: 11087343]
139. Kneuer C, Sameti M, Haltner EG, Schiestel T, Schirra H, Schmidt H, Lehr CM. Int. J. Pharm. 2000; 196:257–261. [PubMed: 10699731]
140. Csogor Z, Nacken M, Sameti M, Lehr CM, Schmidt H. Mater. Sci. Eng. C. 2003; 23:93–97.
141. Sameti M, Bohr G, Kumar M, Kneuer C, Bakowsky U, Nacken M, Schmidt H, Lehr CM. Int. J. Pharm. 2003; 266:51–60. [PubMed: 14559393]
142. Roy I, Ohulchanskyy TY, Bharali DJ, Pudavar HE, Mistretta RA, Kaur N, Prasad PN. Proc. Natl. Acad. Sci. 2005; 102:279–284. [PubMed: 15630089]
143. Peng J, He X, Wang K, Tan W, Li H, Xing X, Wang Y. Nanomed.-Nanotechnol. Biol. Med. 2006; 2:113–120.
144. Choi EW, Koo HC, Shin IS, Chae YJ, Lee JH, Han SM, Lee SJ, Bhang DH, Park YH, Lee CW, Youn HY. Exp. Hematol. 2008; 36:1091–1097. [PubMed: 18550260]
145. Choi EW, Shin IS, Chae YJ, Koo HC, Lee JH, Chung TH, Park YH, Kim DY, Hwang CY, Lee CW, Youn HY. Exp. Hematol. 2008; 36:807–815. [PubMed: 18375041]
146. Bhakta G, Sharma RK, Gupta N, Cool S, Nurcombe V, Maitra A. Nanomed.-Nanotechnol. Biol. Med. 2011; 7:472–479.
147. Zhu SG, Xiang JJ, Li XL, Shen SR, Lu HB, Zhou J, Xiong W, Zhang BC, Nie XM, Zhou M, Tang K, Li GY. Biotechnol. Appl. Biochem. 2004; 39:179–187. [PubMed: 15032738]
148. Sarojini HII, Medepalli K, Terry DA, Alphenaar BW, Wang E. BioTechniques. 2007; 43 213−+
149. Miyata K, Gouda N, Takemoto H, Oba M, Lee Y, Koyama H, Yamasaki Y, Itake K, Nishiyama N, Kataoka K. Biomaterials. 2010; 31:4764–4770. [PubMed: 20304483]
150. Cabral H, Matsumoto Y, Mizuno K, Chen Q, Murakami M, Kimura M, Terada Y, Kano MR, Miyazono K, Uesaka M, Nishiyama N, Kataoka K. Nat. Nanotechnol. 2011; 6:815–823. [PubMed: 22020122]
151. Moudgil S, Ying JY. Adv. Mater. 2007; 19 3130−+
152. Suma T, Miyata K, Anraku Y, Watanabe S, Christie RJ, Takemoto H, Shioyama M, Gouda N, Ishii T, Nishiyama N, Kataoka K. ACS Nano. 2012; 6:6693–6705. [PubMed: 22835034]

153. Gouda N, Miyata K, Christie RJ, Suma T, Kishimura A, Fukushima S, Nomoto T, Liu XY, Nishiyama N, Kataoka K. Biomaterials. 2013; 34:562–570. [PubMed: 23083934]
154. Liu JW, Stace-Naughton A, Brinker CJ. Chem. Commun. 2009:5100–5102.
155. Vanblaaderen A, Vrij A. Langmuir. 1992; 8:2921–2931.
156. Nyffenegger R, Quellet C, Ricka J. J. Colloid Interface Sci. 1993; 159:150–157.
157. Wang L, Wang KM, Santra S, Zhao XJ, Hilliard LR, Smith JE, Wu JR, Tan WH. Anal. Chem. 2006; 78:646–654.
158. Accomasso L, Rocchietti EC, Raimondo S, Catalano F, Alberto G, Giannitti A, Minieri V, Turinetto V, Orlando L, Saviozzi S, Caputo G, Geuna S, Martra G, Giachino C. Small. 2012; 8:3192–3200. [PubMed: 22821625]
159. Sharma P, Bengtsson NE, Walter GA, Sohn HB, Zhou GY, Iwakuma N, Zeng HD, Grobmyer SR, Scott EW, Moudgil BM. Small. 2012; 8:2856–2868. [PubMed: 22744832]
160. Bae SW, Tan WH, Hong JI. Chem. Commun. 2012; 48:2270–2282.
161. Hayashi K, Nakamura M, Ishimura K. Chem. Commun. 2012; 48:3830–3832.
162. Santra S, Yang H, Dutta D, Stanley JT, Holloway PH, Tan WH, Moudgil BM, Mericle RA. Chem. Commun. 2004:2810–2811.
163. Zhao X, Bagwe RP, Tan W. Adv. Mater. 2004; 16:173–176.
164. Santra S, Dutta D, Moudgil BM. Food Bioprod. Process. 2005; 83:136–140.
165. Santra S, Liesenfeld B, Dutta D, Chatel D, Batich CD, Tan WH, Moudgil BM, Mericle RA. J. Nanosci. Nanotechnol. 2005; 5:899–904. [PubMed: 16060150]
166. Choi JH, Burns AA, Williams RM, Zhou ZX, Flesken-Nikitin A, Zipfel WR, Wiesner U, Nikitin AY. J. Biomed. Opt. 2007; 12 064007.
167. Shi H, He XX, Wang KM, Yuan Y, Deng K, Chen JY, Tan WH. Nanomed.-Nanotechnol. Biol. Med. 2007; 3:266–272.
168. Qian J, Li X, Wei M, Gao XW, Xu ZP, He SL. Optics Express. 2008; 16:19568–19578. [PubMed: 19030044]
169. Cao F, Deng RP, Liu DP, Song SY, Wang S, Su SQ, Zhang HJ. Dalton Trans. 2011; 40:4800–4802. [PubMed: 21455503]
170. Guo XM, Guo B, Sun XM, Zhang QY, Shi TS. Chin. J. Chem. 2011; 29:363–368.
171. Kim J, Cao L, Shvartsman D, Silva EA, Mooney DJ. Nano Lett. 2011; 11:694–700. [PubMed: 21192718]
172. He X, Chen J, Wang K, Qin D, Tan W. Talanta. 2007; 72:1519–1526. [PubMed: 19071792]
173. Rendon N, Bourdolle A, Baldeck PL, Le Bozec H, Andraud C, Brasselet S, Coperet C, Maury O. Chem. Mater. 2011; 23:3228–3236.
174. Wu WB, Liu C, Wang ML, Huang W, Zhou SR, Jiang W, Sun YM, Cui YP, Xu CX. J. Solid State Chem. 2009; 182:862–868.
175. Law WC, Yong KT, Roy I, Xu G, Ding H, Bergey EJ, Zeng H, Prasad PN. J. Phys. Chem. C. 2008; 112:7972–7977.
176. Wang XH, Morales AR, Urakami T, Zhang LF, Bondar MV, Komatsu M, Belfield KD. Bioconjug. Chem. 2011; 22:1438–1450. [PubMed: 21688841]
177. Nakamura M, Ozaki S, Abe M, Matsumoto T, Ishimura K. J. Mater. Chem. 2011; 21:4689–4695.
178. Le Guevel X, Hotzer B, Jung G, Schneider M. J. Mater. Chem. 2011; 21:2974–2981.
179. Kumar R, Ding H, Hu R, Yong KT, Roy I, Bergey EJ, Prasad PN. Chem. Mater. 2010; 22:2261–2267.
180. Wang M, Mi CC, Zhang YX, Liu JL, Li F, Mao CB, Xu SK. J. Phys. Chem. C. 2009; 113:19021–19027.
181. Puvanakrishnan P, Park J, Diagaradjane P, Schwartz JA, Coleman CL, Gill-Sharp KL, Sang KL, Payne JD, Krishnan S, Tunnell JW. J. Biomed. Opt. 2009; 14 024044.
182. Mader H, Li X, Saleh S, Link M, Kele P, Wolfbeis OS. Ann. N. Y. Acad. Sci. 2008; 1130:218–223. [PubMed: 18596351]
183. Tan H, Zhang Y, Wang M, Zhang ZX, Zhang XH, Yong AM, Wong SY, Chang AYC, Chen ZK, Li X, Choolani M, Wang J. Biomaterials. 2012; 33:237–246. [PubMed: 21963283]

184. He XX, Wang YS, Wang KM, Chen M, Chen SY. Anal. Chem. 2012; 84:9056–9064. [PubMed: 23017033]
185. Jun BH, Hwang DW, Jung HS, Jang J, Kim H, Kang H, Kang T, Kyeong S, Lee H, Jeong DH, Kang KW, Youn H, Lee DS, Lee YS. Adv. Funct. Mater. 2012; 22:1843–1849.
186. Gerion D, Herberg J, Bok R, Gjersing E, Ramon E, Maxwell R, Kurhanewicz J, Budinger TF, Gray JW, Shuman MA, Chen FF. J. Phys. Chem. C. 2007; 111:12542–12551.
187. Hu KW, Jhang FY, Su CH, Yeh CS. J. Mater. Chem. 2009; 19:2147–2153.
188. Lee YC, Chen DY, Dodd SJ, Bouraoud N, Koretsky AP, Krishnan KM. Biomaterials. 2012; 33:3560–3567. [PubMed: 22341582]
189. Tan H, Wang M, Yang CT, Pant S, Bhakoo KK, Wong SY, Chen ZK, Li X, Wang J. Chem.-Eur. J. 2011; 17:6696–6706. [PubMed: 21542037]
190. Yang J, Lee J, Kang J, Chung CH, Lee K, Suh JS, Yoon HG, Huh YM, Haam S. Nanotechnology. 2008; 19 075610.
191. Cho YS, Yoon TJ, Jang ES, Hong KS, Lee SY, Kim OR, Park C, Kim YJ, Yi GC, Chang K. Cancer Lett. 2010; 299:63–71. [PubMed: 20826046]
192. Park K-S, Tae J, Choi B, Kim Y-S, Moon C, Kim S-H, Lee H-S, Kim J, Kim J, Park J, Lee J-H, Lee JE, Joh J-W, Kim S. Nanomed.-Nanotechnol. Biol. Med. 2010; 6:263–276.
193. Patel D, Kell A, Simard B, Deng JX, Xiang B, Lin HY, Gruwel M, Tian GH. Biomaterials. 2010; 31:2866–2873. [PubMed: 20053440]
194. Heitsch AT, Smith DK, Patel RN, Ress D, Korgel BA. J. Solid State Chem. 2008; 181:1590–1599. [PubMed: 19578476]
195. Ji XJ, Shao RP, Elliott AM, Stafford RJ, Esparza-Coss E, Bankson JA, Liang G, Luo ZP, Park K, Markert JT, Li C. J. Phys. Chem. C. 2007; 111:6245–6251.
196. Kumar R, Roy I, Ohulchanskky TY, Vathy LA, Bergey EJ, Sajjad M, Prasad PN. ACS Nano. 2010; 4:699–708. [PubMed: 20088598]
197. Pinho SLC, Faneca H, Geraldes C, Delville MH, Carlos LD, Rocha J. Biomaterials. 2012; 33:925–935. [PubMed: 22035824]
198. Xing HY, Bu WB, Zhang SJ, Zheng XP, Li M, Chen F, He QJ, Zhou LP, Peng WJ, Hua YQ, Shi JL. Biomaterials. 2012; 33:1079–1089. [PubMed: 22061493]
199. Hu H, Zhou H, Du J, Wang Z, An L, Yang H, Li F, Wu H, Yang S. J. Mater. Chem. 2011; 21:6576–6583.
200. Liberman A, Martinez HP, Ta CN, Barback CV, Mattrey RF, Kono Y, Blair SL, Trogler WC, Kummel AC, Wu Z. Biomaterials. 2012; 33:5124–5129. [PubMed: 22498299]
201. Chen YS, Frey W, Kim S, Kruizinga P, Homan K, Emelianov S. Nano Lett. 2011; 11:348–354. [PubMed: 21244082]
202. Jokerst JV, Miao Z, Zavaleta C, Cheng Z, Gambhir SS. Small. 2011; 7:625–633. [PubMed: 21302357]
203. Napierska D, Thomassen LCJ, Lison D, Martens JA, Hoet PH. Part. Fibre Toxicol. 2010; 7:39. [PubMed: 21126379]
204. Fruijtier-Polloth C. Toxicology. 2012; 294:61–79. [PubMed: 22349641]
205. Marquis BJ, Love SA, Braun KL, Haynes CL. Analyst. 2009; 134:425–439. [PubMed: 19238274]
206. Ema M, Kobayashi N, Naya M, Hanai S, Nakanishi J. Reprod. Toxicol. 2010; 30:343–352. [PubMed: 20600821]
207. Eom HJ, Choi J. Toxicol. in Vitro. 2009; 23:1326–1332. [PubMed: 19602432]
208. Yu T, Greish K, McGill LD, Ray A, Ghandehari H. ACS Nano. 2012; 6:2289–2301. [PubMed: 22364198]
209. Yu T, Malugin A, Ghandehari H. ACS Nano. 2011; 5:5717–5728. [PubMed: 21630682]
210. Oh W-K, Kim S, Choi M, Kim C, Jeong YS, Cho B-R, Hahn J-S, Jang J. ACS Nano. 2010; 4:5301–5313. [PubMed: 20698555]
211. Yuan HH, Gao F, Zhang ZG, Miao LD, Yu RH, Zhao HL, Lan MB. J. Health Sci. 2010; 56:632–640.
212. Zhang YY, Hu L, Yu DH, Gao CY. Biomaterials. 2010; 31:8465–8474. [PubMed: 20701964]

213. Yu KO, Grabinski CM, Schrand AM, Murdock RC, Wang W, Gu BH, Schlager JJ, Hussain SM. J. Nanopart. Res. 2009; 11:15–24.

214. Park MVDZ, Annema W, Salvati A, Lesniak A, Elsaesser A, Barnes C, McKerr G, Howard CV, Lynch I, Dawson KA, Piersma AH, de Jong WH. Toxicol. Appl. Pharmacol. 2009; 240:108–116. [PubMed: 19631676]

215. Quignard S, Mosser G, Boissiere M, Coradin T. Biomaterials. 2012; 33:4431–4442. [PubMed: 22425552]

216. Passagne I, Morille M, Rousset M, Pujalte I, L'Azou B. Toxicology. 2012; 299:112–124. [PubMed: 22627296]

217. Nan AJ, Bai X, Son SJ, Lee SB, Ghandehari H. Nano Lett. 2008; 8:2150–2154. [PubMed: 18624386]

218. Morishige T, Yoshioka Y, Inakura H, Tanabe A, Yao XL, Narimatsu S, Monobe Y, Imazawa T, Tsunoda S, Tsutsumi Y, Mukai Y, Okada N, Nakagawa S. Biomaterials. 2010; 31:6833–6842. [PubMed: 20561679]

219. Chang JS, Chang KLB, Hwang DF, Kong ZL. Environ. Sci. Technol. 2007; 41:2064–2068. [PubMed: 17410806]

220. Brown SC, Kamal M, Nasreen N, Baumuratov A, Sharma P, Antony VB, Moudgil BM. Adv. Powder Technol. 2007; 18:69–79.

221. Herd HL, Malugin A, Ghandehari H. J. Controlled Release. 2011; 153:40–48.

222. Zhao Y, Sun X, Zhang G, Trewyn BG, Slowing II, Lin VSY. ACS Nano. 2011; 5:1366–1375. [PubMed: 21294526]

223. Rabolli V, Thomassen LCJ, Princen C, Napierska D, Gonzalez L, Kirsch-Volders M, Hoet PH, Huaux F, Kirschhock CEA, Martens JA, Lison D. Nanotoxicology. 2010; 4:307–318. [PubMed: 20795912]

224. Liu X, Sun J. Biomaterials. 2010; 31:8198–8209. [PubMed: 20727582]

225. Ye Y, Liu J, Xu J, Sun L, Chen M, Lan M. Toxicol. in Vitro. 2010; 24:751–758. [PubMed: 20060462]

226. Brunner TJ, Wick P, Manser P, Spohn P, Grass RN, Limbach LK, Bruinink A, Stark WJ. Environ. Sci. Technol. 2006; 40:4374–4381. [PubMed: 16903273]

227. Barnes CA, Elsaesser A, Arkusz J, Smok A, Palus J, Leśniak A, Salvati A, Hanrahan JP, Jong WHd, Dziubałtowska Eb, Ste'pnik M, Rydzyński K, McKerr G, Lynch I, Dawson KA, Howard CV. Nano Lett. 2008; 8:3069–3074. [PubMed: 18698730]

228. Cho MJ, Cho WS, Choi M, Kim SJ, Han BS, Kim SH, Kim HO, Sheen YY, Jeong JY. Toxicol. Lett. 2009; 189:177–183. [PubMed: 19397964]

229. Kim JS, Yoon T-J, Yu KN, Kim BG, Park SJ, Kim HW, Lee KH, Park SB, Lee J-K, Cho MH. Toxicol. Sci. 2006; 89:338–347. [PubMed: 16237191]

230. Souris JS, Lee C-H, Cheng S-H, Chen C-T, Yang C-S, Ho J-a.A, Mou C-Y, Lo L-W. Biomaterials. 2010; 31:5564–5574. [PubMed: 20417962]

231. Nishimori H, Kondoh M, Isoda K, Tsunoda S, Tsutsumi Y, Yagi K. Eur. J. Pharm. Biopharm. 2009; 72:626–629. [PubMed: 19341796]

232. Wu J, Wang C, Sun J, Xue Y. ACS Nano. 2011; 5:4476–4489. [PubMed: 21526751]

233. Yamashita K, Yoshioka Y, Higashisaka K, Mimura K, Morishita Y, Nozaki M, Yoshida T, Ogura T, Nabeshi H, Nagano K, Abe Y, Kamada H, Monobe Y, Imazawa T, Aoshima H, Shishido K, Kawai Y, Mayumi T, Tsunoda S-i, Itoh N, Yoshikawa T, Yanagihara I, Saito S, Tsutsumi Y. Nat. Nanotechnol. 2011; 6:321–328. [PubMed: 21460826]

234. Liu T, Li L, Teng X, Huang X, Liu H, Chen D, Ren J, He J, Tang F. Biomaterials. 2011; 32:1657–1668. [PubMed: 21093905]

235. Thakor AS, Luong R, Paulmurugan R, Lin FI, Kempen P, Zavaleta C, Chu P, Massoud TF, Sinclair R, Gambhir SS. Sci. Transl. Med. 2011; 3 79ra33.

236. Nishimori H, Kondoh M, Isoda K, Tsunoda S, Tsutsumi Y, Yagi K. Eur. J. Pharm. Biopharm. 2009; 72:496–501. [PubMed: 19232391]

237. Nelson SM, Mahmoud T, Beaux M, Shapiro P, McIlroy DN, Stenkamp DL. Nanomed.-Nanotechnol. Biol. Med. 2010; 6:93–102.

238. Malfatti MA, Palko HA, Kuhn EA, Turteltaub KW. Nano Lett. 2012; 12:5532–5538. [PubMed: 23075393]
239. Yu T, Hubbard D, Ray A, Ghandehari H. J. Controlled Release. 2012; 163:46–54.
240. Barandeh F, Nguyen P-L, Kumar R, Iacobucci GJ, Kuznicki ML, Kosterman A, Bergey EJ, Prasad PN, Gunawardena S. PLoS One. 2012; 7:e29424. [PubMed: 22238611]
241. Park JH, Gu L, von Maltzahn G, Ruoslahti E, Bhatia SN, Sailor MJ. Nat. Mater. 2009; 8:331–336. [PubMed: 19234444]
242. Hu LC, Shea KJ. Chem. Soc. Rev. 2011; 40:688–695. [PubMed: 21229131]
243. Shea KJ, Loy DA. Chem. Mater. 2001; 13:3306–3319.
244. Zhao L, Vaupel M, Loy DA, Shea KJ. Chem. Mater. 2008; 20:1870–1876.
245. Zhao LH, Loy DA, Shea KJ. J. Am. Chem. Soc. 2006; 128:14250–14251. [PubMed: 17076486]
246. Shea KJ, Loy DA. MRS Bull. 2001; 26:368–376.
247. Khiterer M, Shea KJ. Nano Lett. 2007; 7:2684–2687. [PubMed: 17655368]
248. Pek YS, Wan ACA, Shekaran A, Zhuo L, Ying JY. Nat. Nanotechnol. 2008; 3:671–675. [PubMed: 18989333]

Highlights

- Controlled synthesis of size- and shape-specific silica nanomaterials
- Silica nanoparticles for drug, protein and gene delivery
- Silica nanoparticles for imaging and diagnosis
- Safety of silica nanomaterials

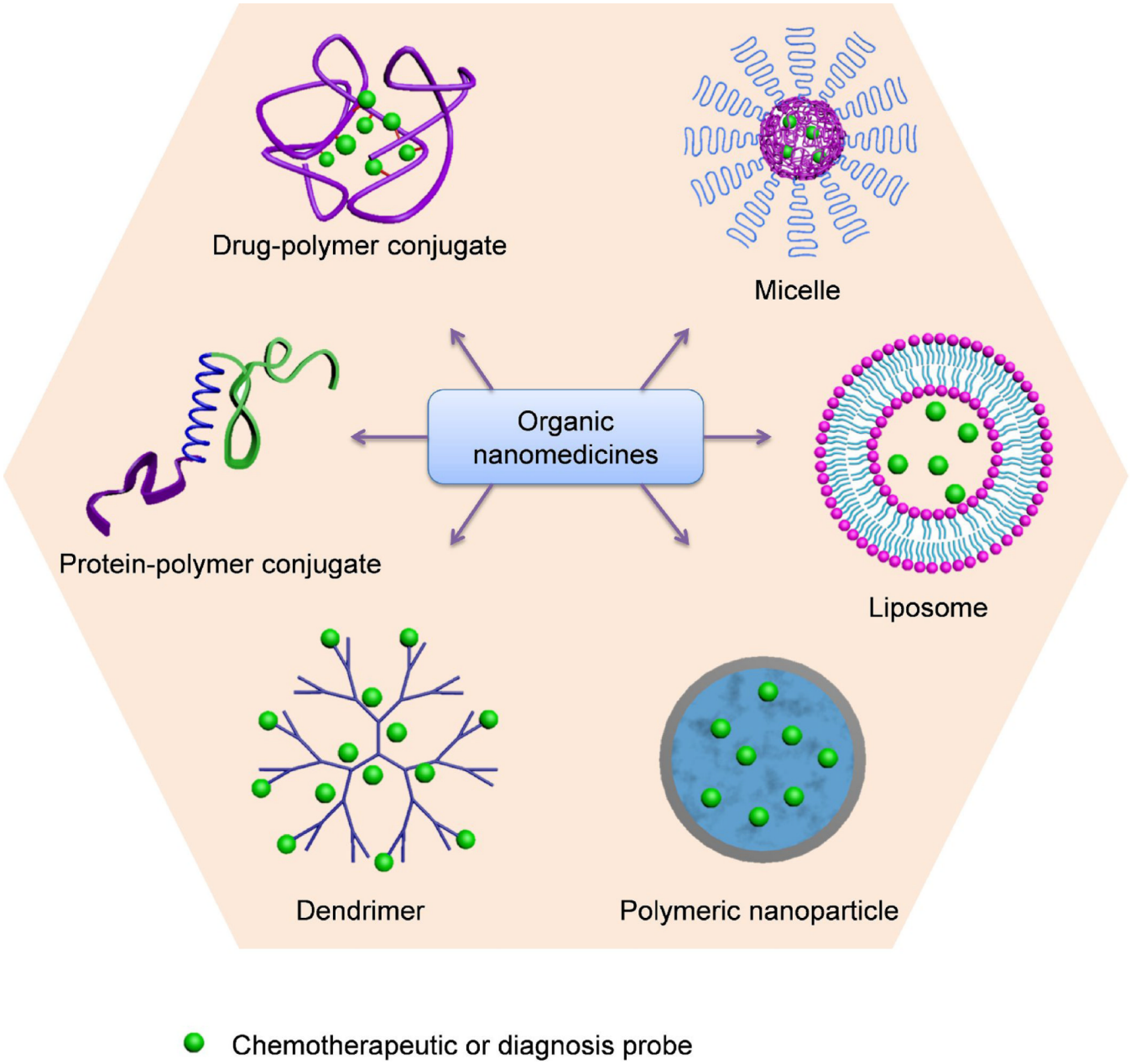

Figure 1.
Examples of organic nanomedicines for cancer diagnosis and therapy.

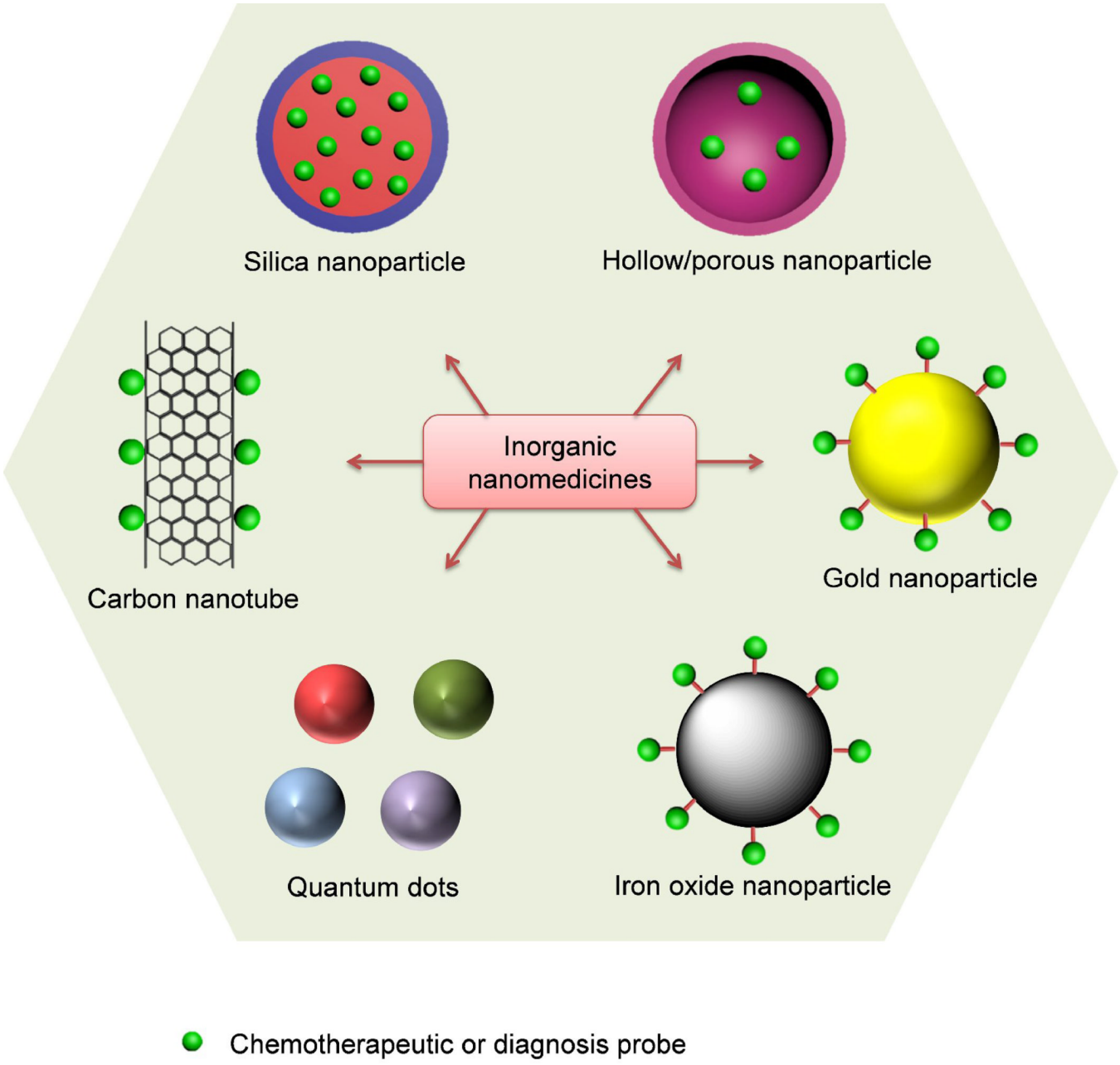

Figure 2.
Examples of inorganic nanomedicines for cancer diagnosis and therapy.

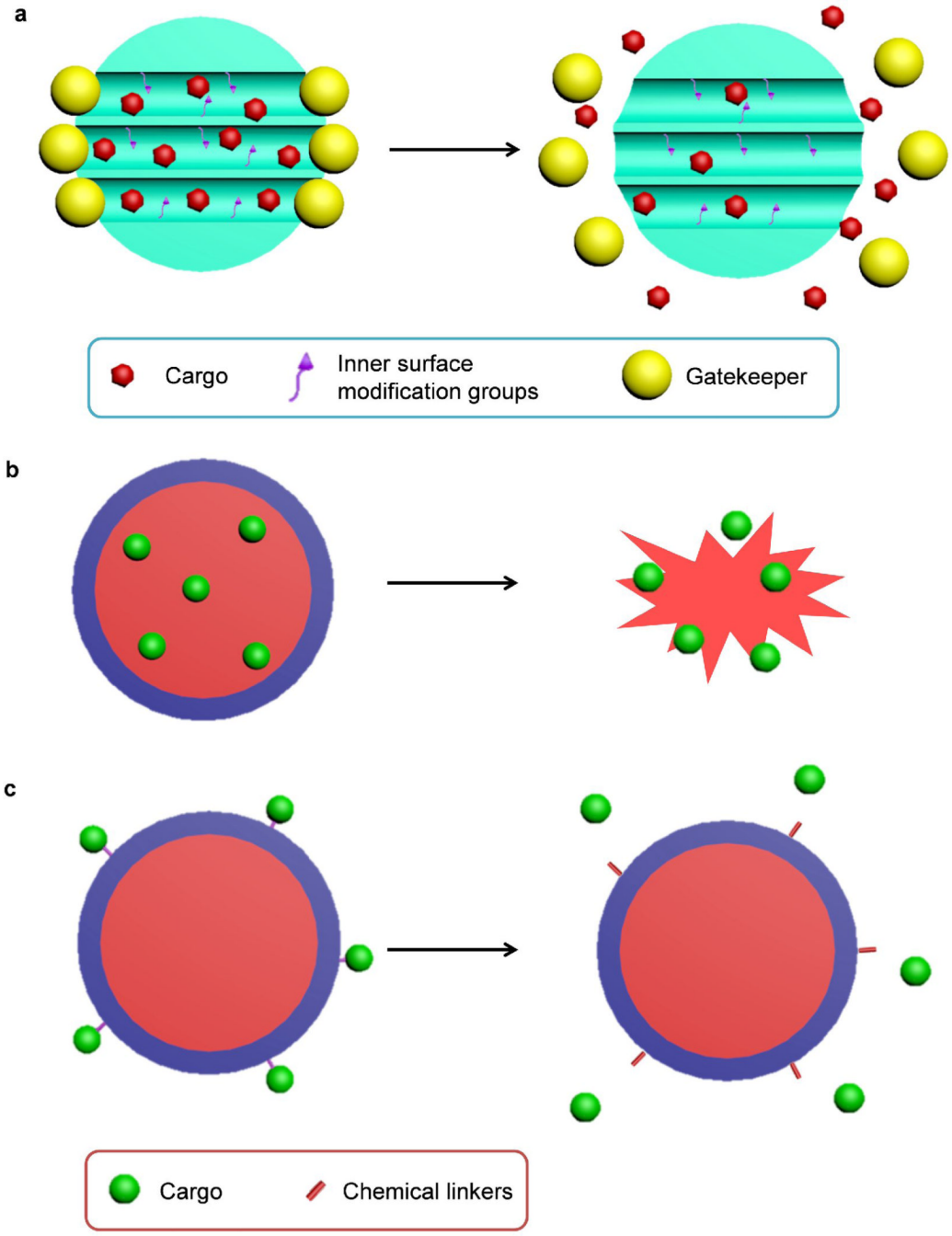

Figure 3.
Schematic diagram of the drug loading and releasing processes in mesoporous silica nanoparticles (NPs) (a) or nonporous silica NPs (b, c). (a) Mesoporous silica NPs are loaded with cargo molecules entrapped in the interior of the nanochannels (meso pores). The inner surface can be modified to control the binding affinity with cargos. Gatekeepers (e.g., gold NPs) are attached to mesoporous silica NP surface for capping to prevent premature release. Cargo release can be facilitated by detaching the gatekeeper with stimuli. (b) Cargos could be encapsulated inside nonporous silica NPs and are released when the silica matrix is degraded. (c) Cargos could also be conjugated with nonporous silica NPs through various

chemical linkers. The release profile of cargos is controlled by the responsive degradation of the chemical linkers.

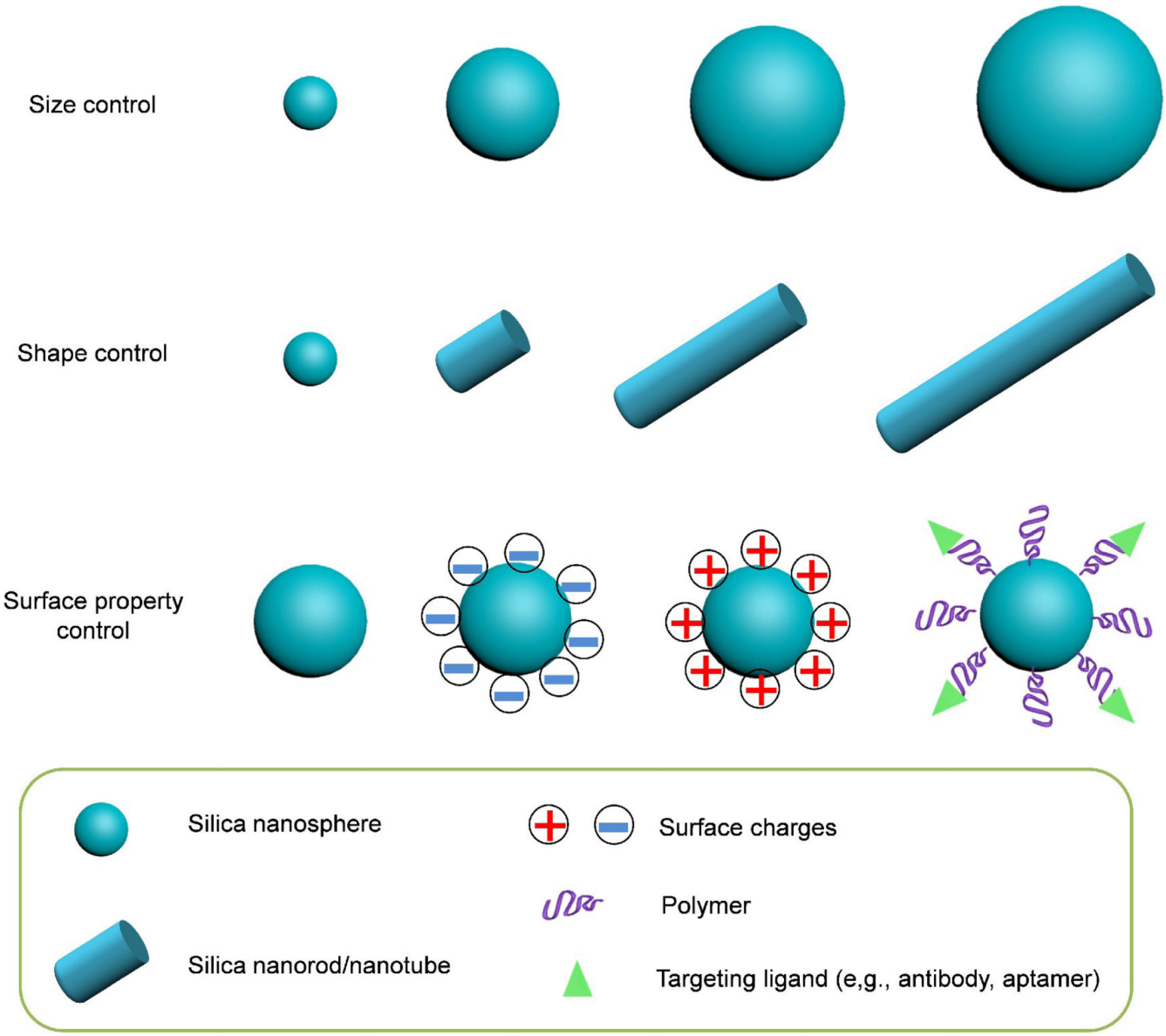

Figure 4.
Schematic representation of the controlled physicochemical properties of silica nanoparticles.

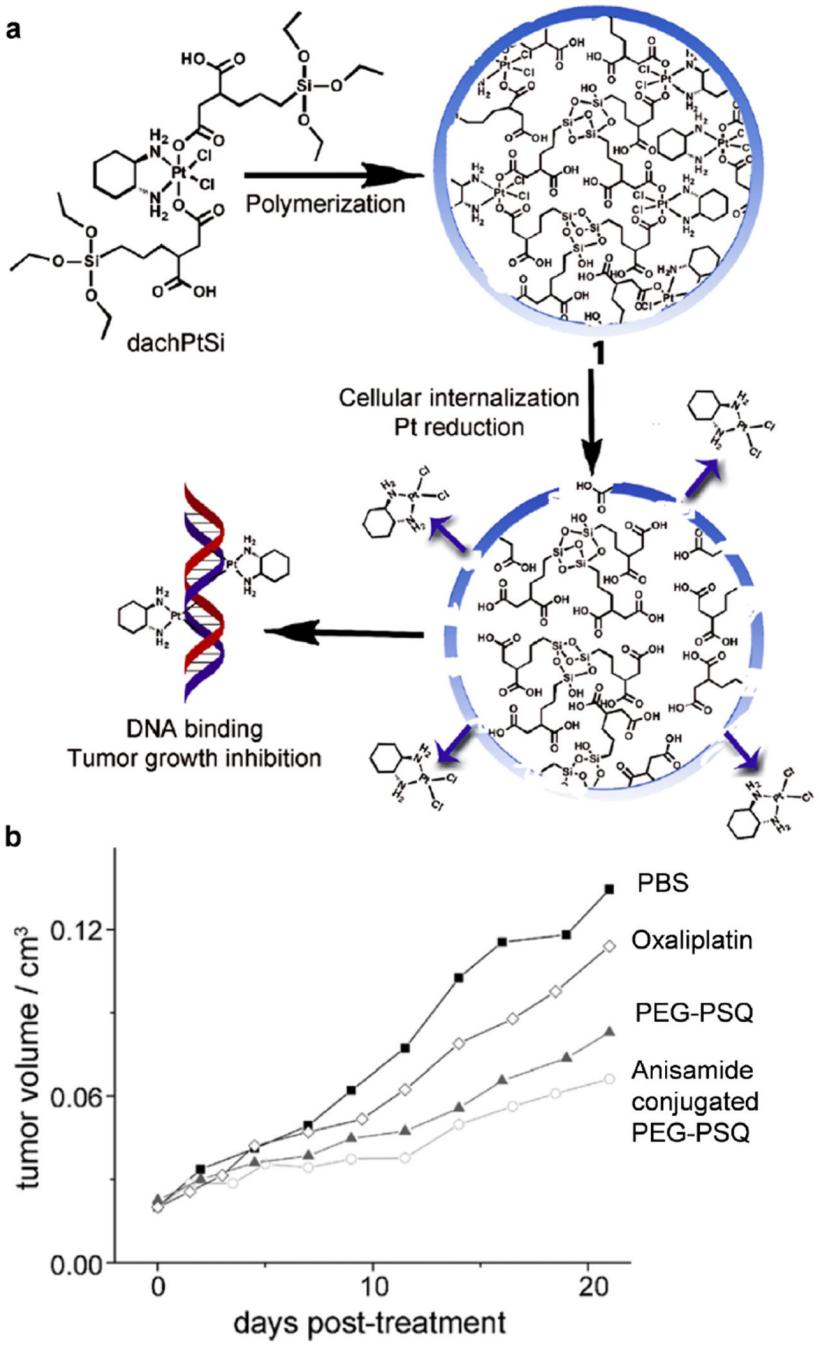

Figure 5.

Polysilsesquioxane nanoparticles for targeted platin-based Cancer chemotherapy. (a) Generalized scheme showing the formation of polysilsesquioxane nanoparticles (PSQ) from the Pt(IV) precursor, dachPtSi. Upon cellular internalization and reaction with endogenous biomolecules, the Pt(IV) complexes in PSQ will be reduced, thereby releasing the active Pt(II) agent. (b) Tumor growth inhibition curves. Mice were administered at 5 mg Pt/kg on days 0, 7, and 14 against an AsPC-1 subcutaneous mouse xenograft. Abbreviations chPtSi:Pt(dach)Cl_2(triethoxysilylpropylsuccinate)$_2$ (dach = *R,R*-diaminocyclohexane); PBS, phosphate buffered saline; PEG, polyethylene glycol; PEG-PSQ, surface PEGylated PSQ.

(Reprinted with permission from Ref [103]. Copyright 2011 Wiley-VCH Verlag GmbH & Co [Angewandte Chemie-International Edition].)

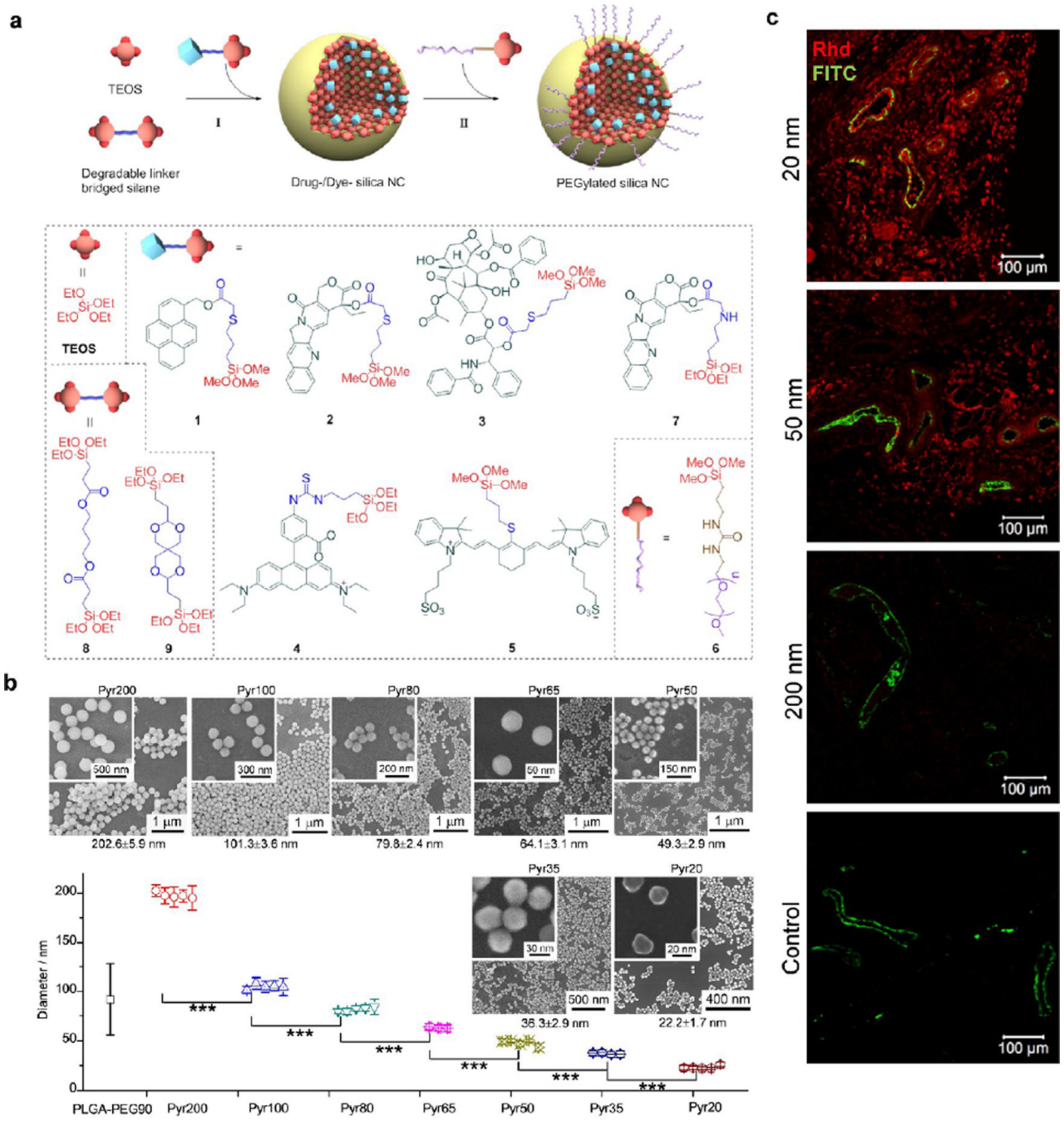

Figure 6.

Precisely size controlled drug-silica nanoconjugates (NCs) for cancer therapy. (a) Schematic showing of the preparation of drug/dye-silica NCs. NCs conjugated with anticancer drugs (camptothecin, paclitaxel) or fluorescence dyes (rhodamine, IR783) are prepared and PEGylated in situ. (b) Preparation of pyrene-silica nanoconjugate (Pyr-NC) with discrete sizes ranging from 20 nm to 200 nm. Three to five independent batches of Pyr-NCs (denoted as PyrX, X = the diameter of NC in nm) were prepared with high consistence for each size. Diameter of NCs was measured via scanning electron microscope images (average ± SD, >100 NCs were counted for each batch). The difference of NC diameters between each size group is highly statistically significant (Student's t-test (two-tailed), ***p-values < 0.001).

The SEM image of each sized NC is shown with a zoom in image inserted. PLGA-PEG NPs of 90 nm in size formed via nanoprecipitation method is compared. (c) C57BL/6 mice bearing Lewis lung carcinoma (LLC) tumors (size: ~5.0 mm × 6.0 mm) were injected intravenously with rhodamine (Rhd)-silica NCs (20, 50 and 200 nm in size). Mice were euthanized and dissected 24 hours post injection. Tumor sections (intersections, 5 μm in thickness) were collected in papraffin and mounted on glass slides and stained for blood vessels. Fluorescence images were taken by Zeiss LSM 700 confocal microscope. Representative two-color composite images show the perivascular distribution of Rhd-silica NCs (red, Rhd channel) in relation to blood vessels (green, FITC channel) in tissue sections of LLC tumors. Abbreviations: TEOS, tetraethyl orthosilicate; PEG, polyethylene glycol; Pyr, pyrenemethanol; PLGA-PEG, poly(lactic-co-glycolic acid)-*b*-polyethylene glycol copolymer. (Reprinted with permission from Ref [104]. Copyright 2012 American Chemical Society [ACS Nano].)

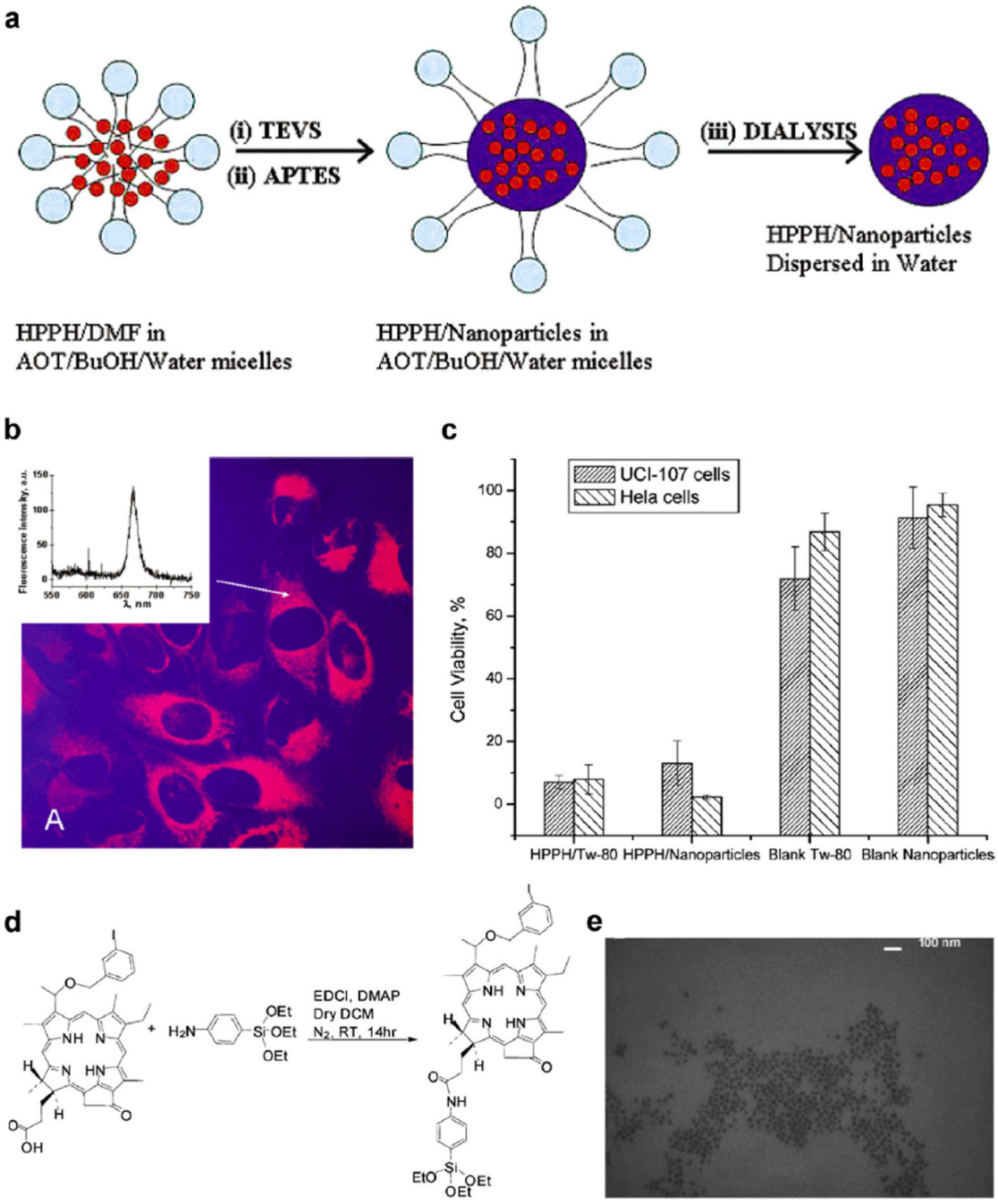

Figure 7.

Silica nanoparticles (NPs) for photodynamic therapy. (a–c) Silica NPs with encapsulated photosensitizing anticancer drug. (a) Scheme depicting the synthesis and purification of HPPH-doped silica-based NPs in a micellar medium. (b) Confocal fluorescence image of HeLa cells treated with HPPH-doped silica NPs. Transmission (blue) and fluorescence (red) channels are shown. Inset: Localized fluorescence spectra from the cytoplasm of the treated cell. Excitation is at 532 nm. (c) Percentage of cell survival of UCI-107 and Hela cells, after treatment with various samples and subsequent irradiation with 650 nm laser light (with reference to irradiated but untreated cells as having 100% survival). Cell viability was assayed by the MTT method (values: mean ± standard deviation). (d–e) Silica NPs with

conjugated photosensitizing anticancer drug. (d) Synthesis of 3-Iodobenzylpyro-silane (IPS), a precursor with the linked photosensitizer iodobenzylpyropheophorbide (IP). (e) Transmission electron microscopy image of the photosensitizer conjugated silica NPs. Abbreviations: HPPH, 2-devinyl-2-(1-hexyloxyethyl)pyropheophorbide; TEVS, triethoxyvinylsilane; APTES, 3-aminopropyltriethoxysilane; DMF, *N,N*-dimethylformamide; BuOH, 1-butanol; AOT, surfactant aerosol OT; MTT, microculture tetrazolium assay; TEM, transmission electron microscopy. (a–c, Reprinted with permission from Ref [30]. Copyright 2003 American Chemical Society [Journal of the American Chemical Society]; d–e, Reprinted with permission from Ref [102]. Copyright 2007 American Chemical Society [Nano Letters])

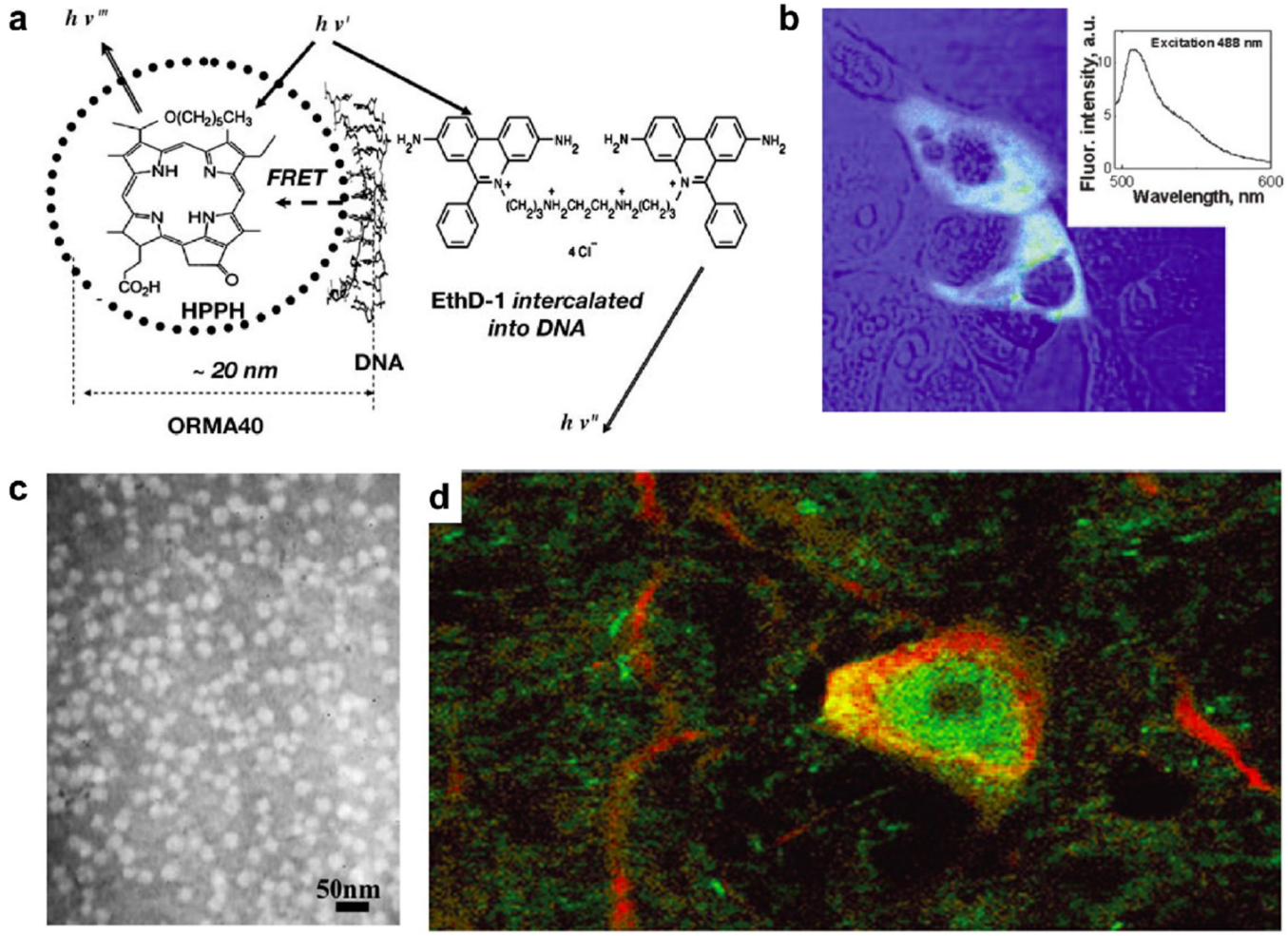

Figure 8.

Organically modified silica nanoparticles (NPs) for gene delivery. (a) The organically modified silica (ORMOSIL) NPs, encapsulating fluorescent dyes (HPPH) and surface functionalized by cationic-amino groups, can efficiently complex with DNA and protect it from enzymatic digestion of DNase1. The scheme represents the FRET occurring as a result of the attachment of DNA labeled with donor fluorophore, ethidium homodimer-1 (EthD-1), to the surface of an ORMOSIL NP containing the encapsulated acceptor fluorophore HPPH. (b) COS-1 cells are transfected with plasmid encoding EGFP delivered with ORMOSIL NPs. A combined transmission (blue) and fluorescence (green) image is shown. Inset: Fluorescence spectra of EGFP taken from cell cytoplasm. (c) Transmission electron micrograph of ORMOSIL NPs that complex with DNA. (d) ORMOSIL NP transfection in the substantia nigra par compacta. Transfected EGFP (green) is expressed in tyrosine hydroxylase-immunopositive (red) dopaminergic neuron. Abbreviations: HPPH, 2-devinyl-2-(1-hexyloxyethyl)pyropheophorbide; FRET, fluorescence resonance energy transfer; EGFP, enhanced green fluorescent protein. (a–b, Reprinted with permission from Ref [142]. Copyright 2005 The National Academy of Sciences of the USA [Proceedings of the National Academy of Sciences of the United States of America]; c–d, Reprinted with permission from Ref [31]. Copyright 2005 The National Academy of Sciences of the USA [Proceedings of the National Academy of Sciences of the United States of America].)

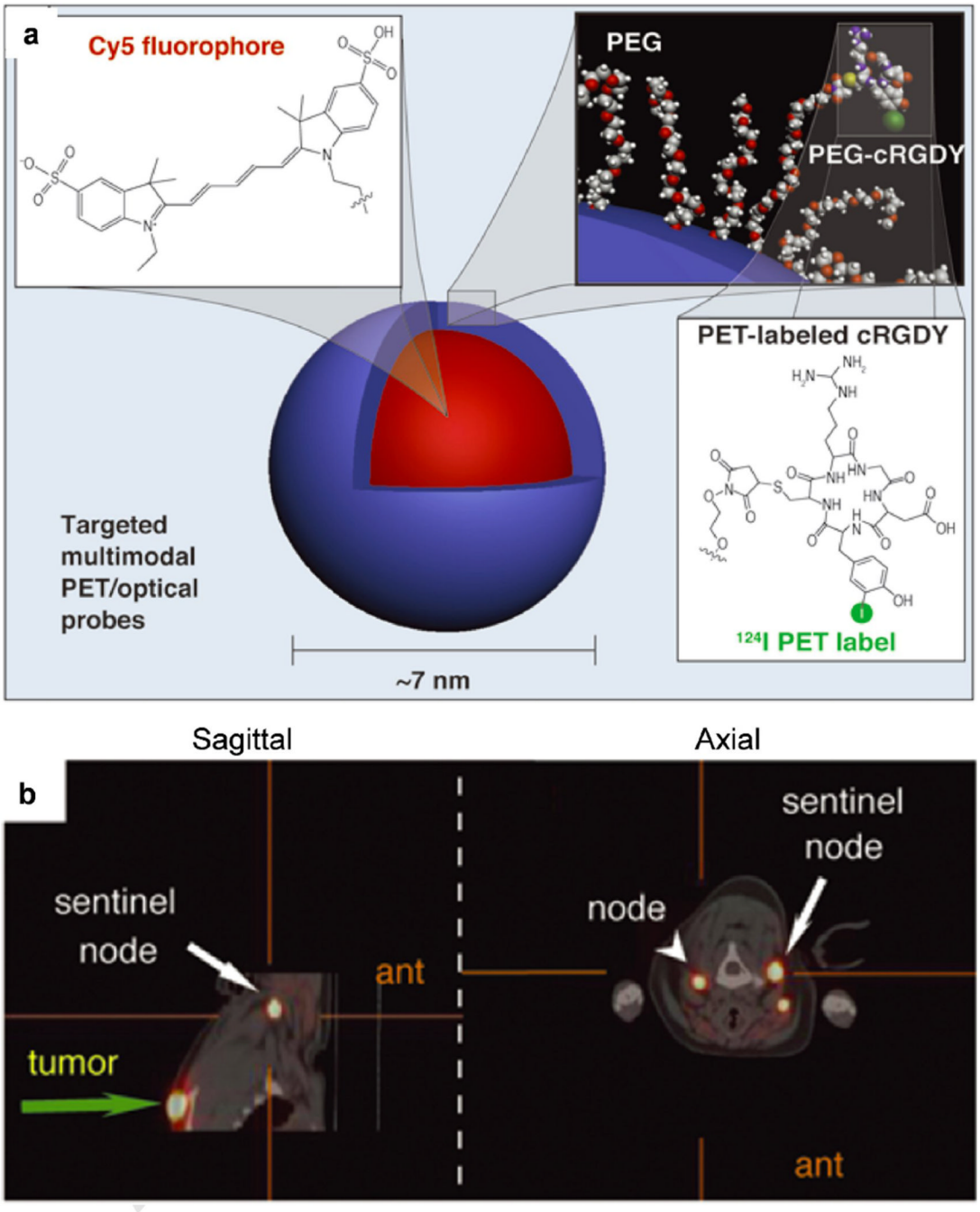

Figure 9.

Multimodal silica nanoparticles for targeted cancer diagnosis in a model of human melanoma. (a) Schematic representation of the ^{124}I-cRGDY-PEGylated core-shell silica nanoparticle with surface-bearing radiolabels and peptides and core-containing reactive dye molecules (insets). (b) High-resolution dynamic PET-CT scan 1 hour after subdermal, 4-quadrant, peritumoral injection of ^{124}I-RGD-PEG-dots. Abbreviations: cRGDY, cyclic arginine–glycine–aspartic acid peptides; PEG, polyethylene glycol; PET, Positron emission tomography; CT, X-ray computed tomography; ant, anterior. (Reprinted with permission from Ref [12]. Copyright 2011 American Society for Clinical Investigation [The Journal of Clinical Investigation]).

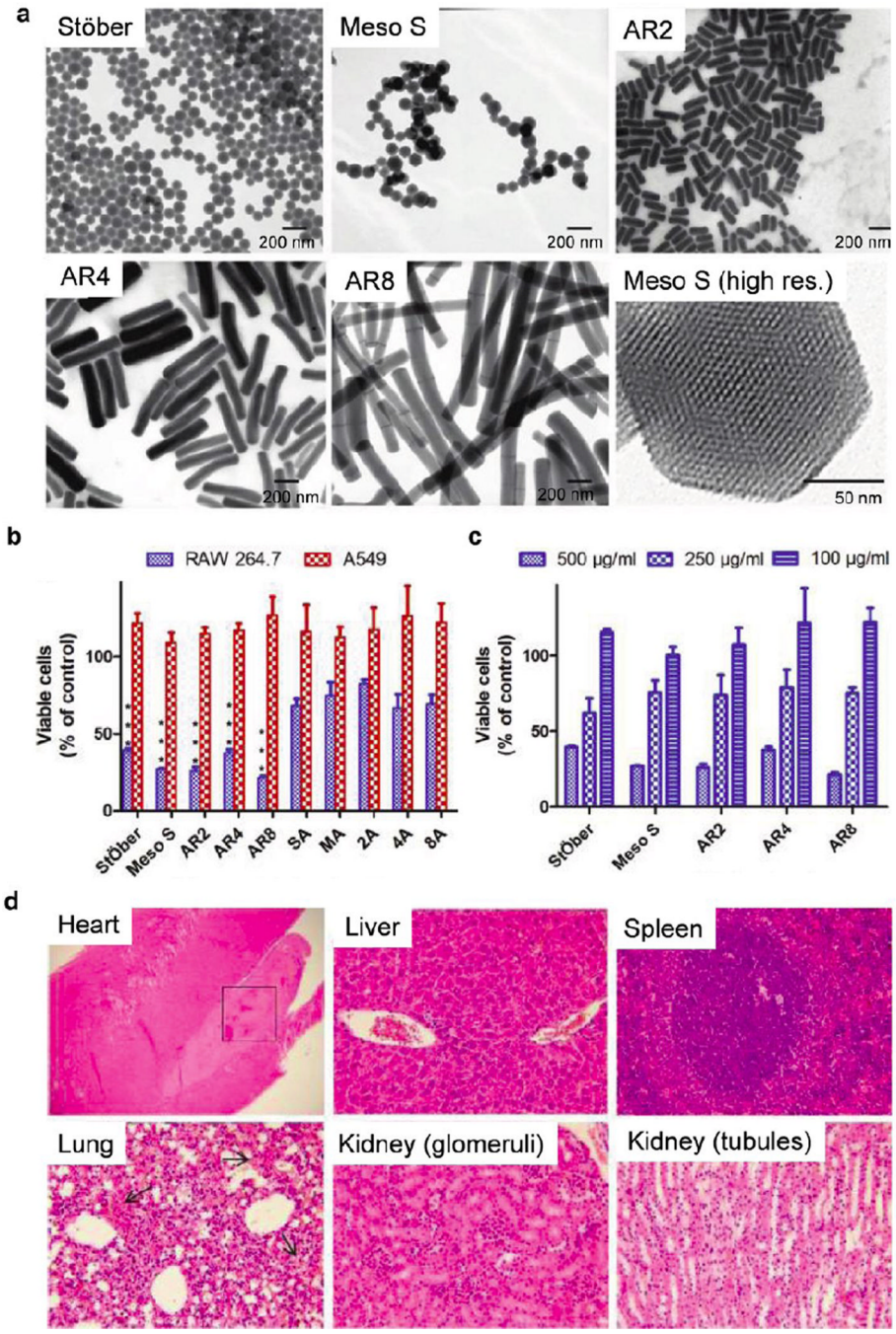

Figure 10.

Influence of geometry, porosity, and surface characteristics of silica nanoparticles (NPs) on *in vitro* and *in vivo* toxicity. (a) Transmission electron microscopy images of Stöber silica NPs with average diameter of 115 nm (referred to as Stöber), mesoporous silica NPs with average diameter of 120 nm (Meso S), mesoporous silica nanorods (NRs) with aspect ratio of 2 (AR2), mesoporous silica NRs with aspect ratio of 4 (AR4), mesoporous silica NRs with aspect ratio of 8 (AR8), and a high-resolution image of a single particle of Meso S. (b–c) Acute cytotoxicity assay. Cells were incubated with bare and amine-modified silica NPs or NRs at 500 μg/mL (b). RAW 264.7 cells were incubated with bare silica NPs or NRs at 500, 250, and 100 μg/mL for 24 h (c). ***: Relative viability of bare silica NP-treated cells

was significantly lower than that of amine-modified counterpart-treated cells ($p < 0.001$). Data are presented as mean ± SD (n = 3). (d) Light microscopic analysis of organs recovered from Stöber silica NP (dose = 600 mg/kg). Arrows in lung sections indicate hemorrhage into the alveoli. All Hematoxylin and eosin staining images were 200× the original magnification except heart tissue image (40 ×). Abbreviations: high res., high resolution. (a–b, Reprinted with permission from Ref [209]. Copyright 2011 American Chemical Society [ACS Nano]; c, Reprinted with permission from Ref [208]. Copyright 2012 American Chemical Society [ACS Nano].)